iJRASET
International Journal For Research in Applied Science and Engineering Technology



INTERNATIONAL JOURNAL FOR RESEARCH

IN APPLIED SCIENCE & ENGINEERING TECHNOLOGY

Volume: 13 **Issue:** VI **Month of publication:** June 2025

DOI: https://doi.org/10.22214/ijraset.2025.72815

www.ijraset.com

Call: 08813907089 | E-mail ID: ijraset@gmail.com

International Journal for Research in Applied Science & Engineering Technology (IJRASET)
ISSN: 2321-9653; IC Value: 45.98; SJ Impact Factor: 7.538
Volume 13 Issue VI June 2025- Available at www.ijraset.com

Innovative Bio retention Strategies: Enhancing Dissolved Nitrogen Removal with Biochar-Amended High-Permeability Media for Urban Storm water Treatment

Debashish Panda[1], Prof. Sanam Sarita Tripathy[2]
[1]*MASTER OF TECHNOLOGY InENVIROMENTAL ENGINEERING GIFTAutonomous, Biju Patnaik University of Technology, Odisha*
[2]*Supervisor, GIFTAutonomous Bhubaneswar Biju Patnaik University of Technology, Odisha*

Abstract: ***Nutrient pollution from stormwater leads inland and coastal water bodies to become eutrophic, which results in sea grass receding and harmful algal blooms (HAB) flourishing. These human-induced effects destabilize the ecosystems, and some HABs threaten human health directly.***
A possible solution to this problem is bioretention, defined as the storage and controlled discharge of storm water runoff in an ecologically constructed setting. But since it is largely reliant on particle settling as a nutrient removal process, it struggles with pollutants such as dissolved nitrogen.
This is particularly inconvenient in India, where nitrogen is the limiting nutrient for HAB growth owing to the geological significance of phosphorus. Several conventional bio retention systems are limited by their low hydraulic loading rates (HLRs) and extensive footprint requirements, rendering them impractical for densely urbanized areas.
To address these constraints, we performed a series of bench-scale, column, and pilot-scale experiments using a novel mixed media of high-permeability gravel amended with biochar. These tests were designed to characterize the hydraulic and physical properties of the amended media, assess its runoff treatment performance under a high HLR representative of extreme precipitation events, and quantify its mass removal efficiency for dissolved nitrogen species at a low HLR corresponding to median storm conditions.
Collectively, these investigations aim to identify a more space-efficient solution capable of handling both extreme and typical storm water loads.
To determine the air-to-water ratio in the soil and assess whether aerobic nitrification or anaerobic denitrification is promoted, HPG was amended with biochar at different volumetric ratios and tested for porosity and moisture retention at the bench scale.
Porosity and moisture-retention capacity increased in direct proportion to the percentage of biochar in the media. Saturated hydraulic conductivity was determined through column tests, and found to be slightly reduced.
This is an indication of decoupling of porosity and saturated hydraulic conductivity, which can be attributed to the internal nanoscale porosity of biochar but still warrants further study.
Finally, two different drain configurations of rain barrels—one with an elevated drain and the other bottom free draining—were utilized to construct pilot-scale bio retention cells.

I. INTRODUCTION

The predominant reason for the spread of HABs that has a deteriorating effect on ecological balance as well as human health is the contamination of nutrients in the nitrogen and phosphorus forms. The HABs directly poison people and/or marine and aquatic life.
Harmful algal blooms (HABs) exacerbate eutrophication in aquatic systems and depress dissolved oxygen concentrations, thereby inhibiting microbial activity (Phlips et al., 2022). Their proliferation is typically constrained by the availability of phosphorus, nitrogen, or both—whichever is in shortest supply—and this limiting nutrient can shift with seasonal changes and across temporal and spatial gradients within an ecosystem (Ding et al., 2018).
Nitrogen loading in aquatic systems arises from sediment desorption, dissolved nitrogen in inflows, and biological fixation from the atmosphere; however, sediment leaching accounts for the bulk of phosphorus inputs (Killberg-Thoreson et al., 2021).

©IJRASET: All Rights are Reserved

Stormwater runoff serves as the principal pathway for both sediment and dissolved nutrient transport, and the proliferation of impervious surfaces in urban areas intensifies these fluxes, complicating mitigation efforts.

The commonly applied storm water control measure called bioretention, which entails harvesting storm water in a filter media-lined basin and delivering it through a control structure, is effective at mitigating the peak flow, volume, and removal of sediment. Dissolved nutrients are, however, challenging for traditional bioretention systems to manage, thereby short-circuiting these systems (Luo et al., 2020).

Additionally, the traditional application ofbioretention systems is compounded by the characteristics of urban watersheds. These systems rely heavily on extended hydraulic retention times (HRT) to ensure adequate treatment quality, which in turn demands large storage capacities. Consequently, they require land areas constituting roughly 25% of the watershed.

Such extensive spatial requirements pose significant challenges in densely populated urban environments, where land availability is limited and property values are high, making these systems less feasible for widespread implementation (Nazarapour et al., 2023). Increased peak flows and reduced lag times are also due to the dominance of impermeable surfaces in such areas.

This enhances run-off variability and complicates the pond sizing due to the low permeability of the filter media, subjecting them to inundation during storms of high frequency or intensity (Burns 2012). The bio retention cell, a smaller system that functions in much the same way as the conventional type, is a modification of traditional bio retention to help solve some of these issues.

By employing high-permeability media, large volumes of urban storm water can be managed within a substantially smaller footprint. More rapid removal of runoff, however, means a smaller HRT and generally lower quality treatment.

An approach to improving the BRS's capacity to control dissolved nutrients is the addition of biochar to the HPG. Biochar is a typical agricultural soil supplement because of its remarkable sorptive and water-holding capacities. It is made by pyrolyzing woodchips and other organic wastes at high temperatures under oxygen-limited circumstances(Reddy et al., 2014).

These systems rely heavily on extended hydraulic retention times (HRT) to ensure adequate treatment quality, which in turn demands large storage capacities. Consequently, they require land areas constituting roughly 25% of the watershed.

Such extensive spatial requirements pose significant challenges in densely populated urban environments, where land availability is limited and property values are high, making these systems less feasible for widespread implementation.

The biochar amendment’s enhanced water retention and adsorption properties should both sequester pollutants and foster microbial biofilm development, thereby driving nitrogen transformations via the biogeochemical cycle and ultimately releasing inert N_2 gas.

We further hypothesized that, whereas a free-draining bio retention system would predominantly support nitrification, one fitted with an elevated outlet to establish an internally saturated zone (IWSZ) would create anaerobic conditions favourable to DE nitrification.

A condition that will promote denitrifying bacteria is established when aeration and oxygen supply are restricted by the buildup of moisture between events.

The primary objective of this study was to comprehensively assess the effectiveness of BRS constructed with biochar-amended high-permeability gravel for the removal of dissolved nitrogen species from stormwater runoff.

The investigation focused not only on total inorganic nitrogen (TIN) removal efficiency but also on the specific pathways of nitrogen transformation, particularly the removal of ammonium (NH_4^+) and oxidized nitrogen species (NO_x).

Furthermore, the study evaluated the impact of varying hydraulic loading rates, comparing conditions representative of a 10-year storm event with a peak hydraulic loading rate of 11.8 cm/min to those of a median-frequency storm at 2.4 cm/min.

Additionally, two distinct drainage configurations—free-draining and raised-drainage systems—were examined to determine their effects on key performance metrics, including runoff volume retention, nitrogen mass removal efficiencies, and the relative contributions of different nitrogen species to the overall treatment process.

This multifaceted approach enabled a thorough understanding of how hydraulic stress and system design influence nitrogen attenuation mechanisms within biochar-amended BRS media.

II. LITERATURE REVIEW

A. Management of Urban Stormwater

1) Variability and the First Flush of Urban runoff

Increase in urbanization profoundly alters watershed hydrology by reshaping flow pathways and disrupting processes such as evapotranspiration and infiltration, thereby modifying stream flow patterns and runoff partitioning (Douglas, 2020). Several uncertainties associated with each phase compound these occurrences.

It is difficult in and of itself to define what constitutes an "urban watershed" because governments worldwide have taken disparate approaches to categorizing land-use, population, and building parameters.

Generation of runoff and storm flashiness augment as the rate of impermeable building increases. For instance, concrete surfaces produce approximately seven to nine times more runoff compared to brick.

The effectiveness of pervious surfaces in urban catchments is strongly influenced by their hydrological connectivity to adjacent impervious areas (McGrane, 2016).

Runoff from impervious zones rapidly saturates adjacent pervious soils, reducing infiltration capacity, hastening runoff onset, and raising the runoff-to-storm intensity ratio—even when the overall impervious fraction remains unchanged.

Guan et al. (2016) investigated the specific-storm-depth threshold of a catchment. Storms that occur below this threshold create nearly no pervious runoff, while storms that occur beyond it can yield a pervious-runoff-to-storm-depth ratio that is up to double that of smaller occurrences. When fully saturated, pervious zones may contribute approximately one-half to two-thirds of peak runoff flows during intense storms (Skaugen et al., 2020).The effects of a watershed can also be significantly altered by the location of impervious regions; according to Du et al. (2015), impervious surfaces located upstream can produce up to fourteen times more runoff than those situated downstream.These effects were substantially more noticeable in smaller catchments, according to Roodsari et al. (2016).

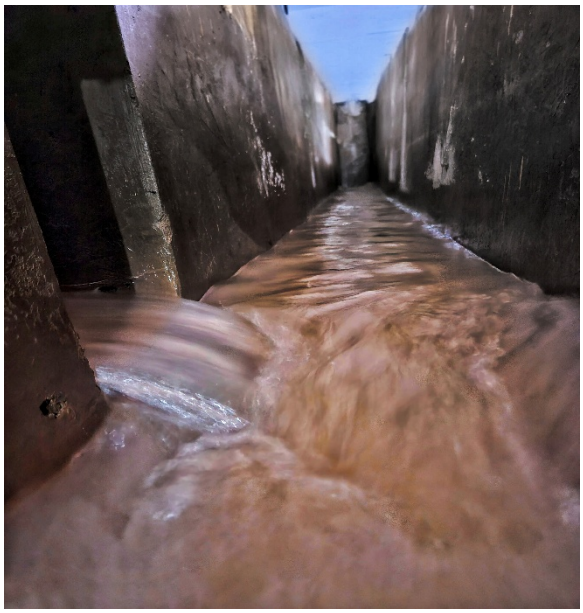
Besides a mean intensity of storm, duration, and total depth, its hyetograph shape must also be considered, since variations in temporal rainfall distribution can markedly affect runoff generation—with storms exhibiting higher peak intensities yielding disproportionately greater runoff (Guan et al., 2015).

Urban storm water diffuse, nonpoint-source nature undermines hydrograph predictability and complicates water-quality control.

Regulations typically require capture of the initial 0.5–1 inch “first flush,” which concentrates surface-washed pollutants, before allowing subsequent, cleaner runoff downstream (Ahlfeld et al., 2004).

Nitrogen and phosphorus drive eutrophication but behave differently: nitrogen is “source-limited,” exhibiting a strong first-flush effect even in small storms, whereas phosphorus is “transport-limited,” with larger events mobilizing greater phosphorus loads (Hathaway et al., 2012; Egodawatta& Goonetilleke, 2008; Vaze & Chiew, 2004). Both nutrients occur in fine particulates (<75 nm) and as dissolved species (DON, NO_3^-, NH_4^+) (Miguntanna et al., 2013).

2) Bio retention for Urban Stormwater Treatment



Accumulation systems are the class of Low Impact Development (LID) practices designed to capture storm water and allow it to infiltrate through a multi-layer filter (Davis et al., 2006). By facilitating groundwater recharge, attenuating peak flows via storage, and enhancing pollutant removal through combined biotransformation and physico-chemical processes, these systems improve both quantity and quality of urban runoff.

Common LID configurations include rain gardens and bioswales, which typically consist of a vegetated or mulch surface underlain by a fine sand layer and finished with a coarse drainage medium (Trowsdale et al., 2011; Ali et al., 2021).
Although nutrient removal—particularly of inorganic nitrogen species—can be inconsistent in these installations (Hsieh et al., 2005Brown et al., 2009), incorporating an internally saturated zone (IWSZ) can create anaerobic conditions that enhance denitrification (Brown et al., 2011).

3) Reduction of Nitrogen and its Removal in Bio retention Cell

Denitrification—reducing nitrate to N_2 under anoxic conditions—is the primary nitrogen removal pathway in bio retention systems, even though aerobic nitrification (converting NH_4^+ to NO_3^-/NO_2^-), anammox (coupling NH_4^+ and NO_2^- to N_2), and assimilation also contribute. By stacking semi-saturated aerobic and fully saturated anaerobic zones in a single soil column, these processes can be integrated to maximize storm water nitrogen stripping (Biswal et al., 2022; Zhang et al., 2021; Zart et al., 2008).

4) Limitations involved withBio retention in Urban Catchments

BRS are tailored to capture target particle sizes and operate at designated HLRs, forcing a trade-off between hydraulic conductivity and treatment performance that is often dictated by space constraints (Laurenson et al., 2013).
Their limited adsorption capacity and high solubility of dissolved nitrogen species hinder effective N removal. Even bio retention designs modified with an internally saturated zone (IWSZ) exhibit improved performance, yet removal efficiencies remain highly variable (Yang et al., 2010; Luo et al., 2020). Urban bio retention can also be further restricted by paucity and expensive land.
As per Nazarapour et al. (2023), the ratio of bio retention area to contributing catchment area can be between 8 and 25%.
Lower rates of infiltration are necessary to lengthen hydraulic residence times enough to effectively improve the quality of storm water, establish a baseline for this number (Wright et al. 2018). Insufficiency of media permeability, contributed by partial errors of incorrect mix proportions and depths of the media and compounded by clogging of organic solid due to the material, was cited by Ray et al. (2015) as the explanation for prolonged ponding of Columbia region bio retention facilities in 2013–2014.

B. Bio retention Cell Design for Nitrogen Reduction in Urban Watersheds

1) Filter Media Characteristics

Bioretention media are typically composed of vegetated layers of sand or gravel, supported by an underlying mulch layer that contributes to organic matter and moisture retention. To maximize hydraulic permeability and minimize volumetric changes caused by swelling or shrinkage, media are often engineered with a high sand content and minimal clay fraction, as clay's expansive nature can reduce permeability and alter pore structure (Brady & Weil, 2002).
While coarser sands facilitate rapid infiltration and drainage, finer particles contribute to enhanced contaminant removal through increased surface area and adsorption capacity. Thus, an optimal balance must be achieved to reconcile permeability and pollutant removal performance.
The effectiveness of bioretention systems (BRS) is strongly governed by several interrelated factors. Media depth influences the contact time and the volume of water retained, while the configuration and layering of different material strata affect flow paths, retention zones, and redox conditions critical for biochemical reactions such as denitrification.
Particle size heterogeneity within the media creates a complex pore network that governs infiltration rates, retention capacity, and microbial habitat quality (Hsieh et al., 2005).
Recent research by Reddy et al. (2021) highlights that blending sand with various sorptive amendments—including biochar, iron oxides, or activated carbon—can achieve nitrate removal efficiencies that are comparable to or surpass those attained by layered but unmixed media configurations.
This blending promotes greater uniformity in contaminant contact and reactive surface distribution. Moreover, layering materials with distinct hydraulic conductivities can establish favorable hydrologic gradients and promote anoxic zones necessary for anaerobic denitrification processes.
For example, placing a lower-permeability sand layer beneath a more permeable upper layer slows water movement, increasing residence time and sustaining reducing conditions, even in the absence of an engineered internal water storage zone (Luo et al., 2020).
Bioretention media generally display saturated hydraulic conductivities ranging between 5 and 600 mm/hr (approximately 0.0083 to 1 cm/min).

©IJRASET: All Rights are Reserved | SJ Impact Factor 7.538 | ISRA Journal Impact Factor 7.894 |

Exceeding this upper limit can adversely affect plant water uptake efficiency by reducing soil moisture retention and nutrient availability, thereby potentially compromising vegetation health and system performance (Laurenson et al., 2013).

Further, according to guidelines from the American Society of Civil Engineers (ASCE), sorptive materials designed specifically for stormwater treatment applications exhibit a wide spectrum of specific surface areas—from as low as 0.05 m^2/g to as high as 27 m^2/g—indicative of their varying adsorption capacities and reactivities (Liu et al., 2001). This variability underscores the importance of carefully selecting media based on site-specific treatment goals, pollutant loadings, and hydraulic requirements to optimize both contaminant removal and hydraulic function.

a) Biochar

Biochar is a highly porous sorbent material produced through the thermal decomposition of organic biomass in an oxygen-limited environment, a process known as pyrolysis. This thermal conversion typically occurs at temperatures up to approximately 1000 °C and results in a carbon-rich, stable product with a complex pore structure.

The unique physical characteristics of biochar—specifically its extensive surface area and high porosity—make it an effective amendment for soil and engineered media, influencing both hydrological and chemical soil properties.

When incorporated into natural soils or substrate media, biochar has the potential to significantly modify hydraulic behavior by disrupting the conventional relationship between saturated hydraulic conductivity and particle size distribution. This deviation occurs because biochar's nanoporous architecture contributes to increased total porosity, enhancing water retention capacity without proportionally increasing flow pathways.

The pores within biochar particles can retain water that does not readily contribute to percolation, thus reducing overall hydraulic conductivity despite increased porosity (Chapuis, 2004; Liu et al., 2016). However, it is important to note that the physical and chemical properties of biochar are not uniform and can vary substantially depending on feedstock type, pyrolysis temperature, residence time, and other processing conditions.

For example, higher pyrolysis temperatures generally produce biochars with greater surface area, increased aromaticity, and enhanced structural stability, but may reduce the presence of functional groups important for nutrient retention and cation exchange (Kinney et al., 2012).

This variability complicates the prediction of biochar's exact hydraulic and adsorptive impacts when used as a soil amendment. Among the key physicochemical traits contributing to biochar's adsorption capacity are its specific surface area and cation exchange capacity (CEC).

The specific surface area represents the total available surface for chemical reactions and adsorption and is often measured using techniques such as BET (Brunauer–Emmett–Teller) analysis. CEC refers to the biochar's ability to retain and exchange positively charged ions, which is critical for nutrient retention and pollutant removal.

Studies have documented biochar surface areas ranging up to approximately 100 m^2/g and CEC values around 10 cmol/kg, although these values can differ widely based on production methods and feedstock composition (Rahman, 2021).

b) Bio retention Drain Characteristics

Through their comparison of a few columns with different sand media, both with and without an IWSZ, Huang et al. (2022) found that ammonia was totally converted into nitrate in all configurations. They reported complete nitrification, with ammonia (NH_4^+) fully oxidized to nitrate (NO_3^-) across all tested configurations. Their data further revealed that columns integrating vegetative components alongside an IWSZ exhibited significantly enhanced denitrification efficiency (DE), attributed to the maintenance of anoxic conditions conducive to microbial reduction processes within the IWSZ. Donaghue et al. (2022) investigated the hydraulic influence of drain height placement in columns outfitted with upturned elbow drains forming the IWSZ.

By varying the inlet depth of the drainage pipe, they established top, mid, and bottom-drain configurations, effectively modulating the vertical extent and volume of the IWSZ. As the drain height decreased, the volume of immobile pore water zones within the IWSZ diminished, promoting intensified denitrification by enhancing substrate transport and microbial contact efficiency.

This spatial alteration of hydraulic retention within the pore network was quantitatively supported by tracer studies comparing theoretical hydraulic residence times (HRT) with experimentally measured values in columns featuring elevated drains and inverted elbow geometries.

The results provided critical insights into the interplay between flow dynamics, pore-scale heterogeneity, and nitrogen transformation pathways in engineered bioretention media.

©IJRASET: All Rights are Reserved | SJ Impact Factor 7.538 | ISRA Journal Impact Factor 7.894 |

ISSN: 2321-9653; IC Value: 45.98; SJ Impact Factor: 7.538
Volume 13 Issue VI June 2025- Available at www.ijraset.com

In elevated bioretention systems with an IWSZ characterized by a width-to-depth ratio greater than one, as well as higher HLRs, mixing between fresh inflow and aged water in the IWSZ is intensified, thereby reducing immobile water regions.
Under such conditions, Donaghue (2022) observed that raised drainage configurations exhibit approximately 25% shorter HRTs compared to inverted drains. By minimizing immobile pore spaces within the IWSZ, a larger proportion of anaerobic water is exchanged and renewed between rainfall events, potentially enhancing the overall contaminant removal efficiency.
Considering these observations, the present study addresses several important gaps in existing research. Specifically, it aims to examine the behavior and performance of bioretention media under extreme hydraulic loading conditions, elucidate how different drainage designs influence IWSZ geometry, investigate coupled nitrification–denitrification occurring within bioinfiltration systems, and assess whether biochar amendments can stimulate microbial remediation processes in otherwise biologically inert substrates.
Additionally, this research seeks to characterize how such amendments impact the hydraulic performance of bioretention systems.

III. MATERIALS AND METHODS

A. Materials

1) High Permeability Gravel (HPG)

For this project, the primary material was a patented high permeability gravel (HPG). As illustrated in Figure 3.1, the media primarily consists of gravel-sized particles and comprises a heterogeneous mixture of various particle sizes and types.
USF was not provided with the product's specific specifications, which are proprietary. All HPG was cleaned prior to any testing or construction with deionisedwater using a 4.75 mm screen to ensure that the medium is free of any foreign objects and to avoid precipitation of minerals or ions from the tap water.
Additionally, coarse gravel was placed at the base of both the column and pilot-scale systems to establish a free-drainage boundary condition. This gravel was significantly larger in particle size than the high-permeability gravel (HPG) and exhibited correspondingly higher permeability.

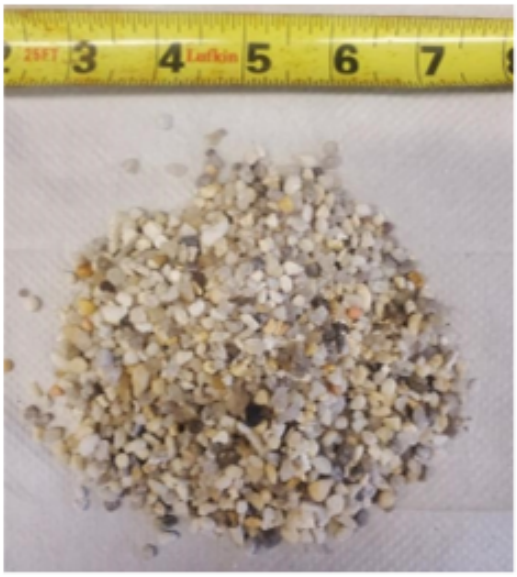


Figure 3. 1 High permeability gravel image to showcase particle diversity

2) Biochar Now (BCN)

The bench-scale study considered two forms of biochar: Biochar (BCS) from Everson, Washington, and Biochar Now (BCN) from Loveland, Colorado. BCS was collected commercially, which was produced in Washington State with ingredients listed by the Organic Components Research Institute (OMRI) and contains a minimum of 70% organic carbon. They say on their website that BCN is produced in Colorado from a wide range of woody material, including beetle-kill and burned trees. They offer several different sizes of aggregates; Figure 3.2 shows the medium chosen for this study.
Both were acceptable to this study and were tested on a bench scale. The material for the pilot scale study was finally decided by availability issues. as BCS ceased to communicate and appeared to reorganize.

©IJRASET: All Rights are Reserved

Rahman (2021) reported specific surface area values of 537 m²/g and 136 m²/g, alongside cation exchange capacity (CEC) values of 10.57 and 13.63 cmol/kg, respectively, based on the characterization of two biochar-amended media types, BCS and BCN.

To ensure purity and prevent the accumulation of minerals or ions from tap water, all collected biochar samples were thoroughly rinsed with deionized water through a 0.05 mm sieve to remove extraneous materials prior to use.



Figure 3. 2 Biochar Now image.

3) Column Study

Three PVC columns, each with a capacity of 1 L, were constructed to assess the hydraulic conductivity and water retention characteristics of high-permeability gravel (HPG) amended with 40% biochar. Two configurations were tested: free-draining and raised-drainage, with unmodified HPG under free-draining conditions serving as the control.

Each column measured 8.255 cm in outer diameter, 7.68 cm in inner diameter, and had a wall thickness of 0.635 cm.

To facilitate detailed sampling, three ports (0.95 cm diameter) were vertically spaced at 10.2 cm intervals along the column length. In the raised-drainage configuration, the base of the column was sealed to prevent free drainage, and a drain line was installed at the lowest sampling port to establish an internal water storage zone (IWSZ).

In contrast, the free-draining columns were left open at their bases, allowing unrestricted outflow. To facilitate effective drainage and prevent media migration, a layer of coarse gravel was placed at the bottom of all columns, separated from the finer media above by a metal screen. A laboratory photograph of the assembled columns is presented in Figure 3.3, while the schematic design of the experimental setup is depicted in Figure 3.4.



Figure 3. 3 Photograph of bench scale column system in the lab

©IJRASET: All Rights are Reserved | SJ Impact Factor 7.538 | ISRA Journal Impact Factor 7.894 |

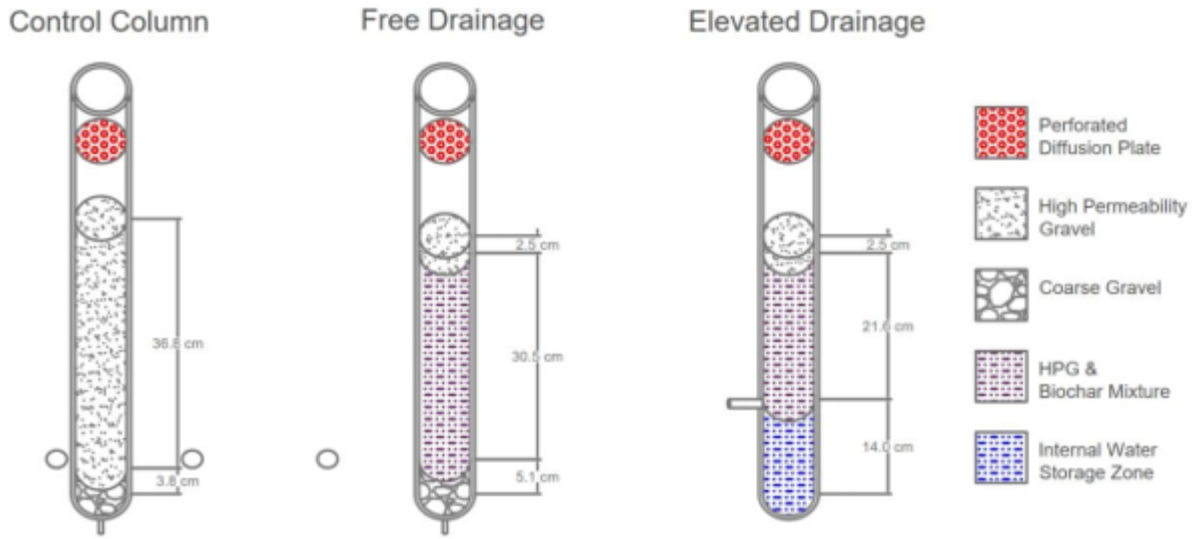
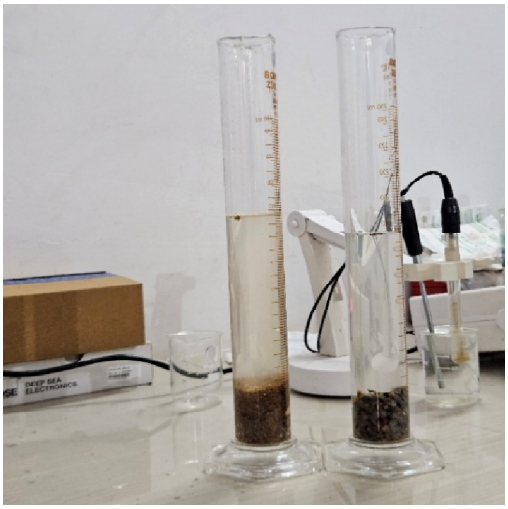


Figure 3. 4 Column system schematic



4) Pilot Study

Two pilot-scale bioretention systems were fabricated using high-density polyurethane barrels at the Mirainbarrel facility (Romulus, MI), designed to investigate the influence of drainage configuration on hydraulic and nitrogen removal performance.

Each system employed a distinct drainage approach—free-drainage and elevated drainage—to simulate differing hydrologic regimes encountered in practical applications.

The free-drainage system was mounted on a custom-fabricated plastic pallet featuring a precision-machined cutout to securely accommodate a 7.6 cm diameter bulkhead fitting. This bulkhead served as a hydraulic interface, permitting effluent discharge through an attached PVC elbow and outlet piping assembly.

At the base of the barrel, a 7.6 cm thick coarse gravel drainage layer was installed to maintain high permeability and prevent clogging. A stainless steel mesh screen was positioned at the bulkhead interface to prevent media loss while allowing unimpeded water flow.

To suppress the upward migration and potential flotation of biochar particles, a 5.1 cm thick cap of unamended high-permeability gravel (HPG) was placed above the primary treatment media, which consisted of a 71.7 cm thick bed of HPG amended with 40% biochar by volume (referred to as BCN). This design facilitated consistent hydraulic contact and mechanical stability during high flow events.

©IJRASET: All Rights are Reserved | SJ Impact Factor 7.538 | ISRA Journal Impact Factor 7.894 |

In contrast, the elevated drainage system utilized a separate barrel equipped with a smaller, 3.81 cm diameter bulkhead fitting, installed approximately 15.2 cm (6 inches) above the barrel base to establish an internal water storage zone (IWSZ).
Attached to this bulkhead was a 50.8 cm long PVC pipe, sealed at the distal end and perforated with an array of 0.318 cm diameter holes spaced evenly along its length to allow controlled effluent drainage.
This configuration created a saturated zone approximately 15.2 cm deep, fostering anoxic conditions conducive to enhanced denitrification. The IWSZ also functioned as a hydraulic buffer, modulating flow rates and residence times within the media column.
Similar to the free-drainage system, a 5.1 cm top layer of untreated HPG was placed over 180.6 cm (71.1 inches) of biochar-amended HPG media to mitigate biochar displacement and maintain structural integrity under varying hydraulic loads.
The entire pilot setup, including the feedwater supply tank and both drainage systems, is documented in the field photograph shown in Figure 3.5.
Additional construction details, including dimensional specifications and component arrangements, are provided in the schematic diagram depicted in Figure 3.6. These designs facilitate controlled investigation of flow dynamics, nitrogen transformations, and hydraulic performance under conditions representative of urban stormwater treatment scenarios.



Figure 3. 5 Photograph of feedwater tank and pilot BRSs in the field

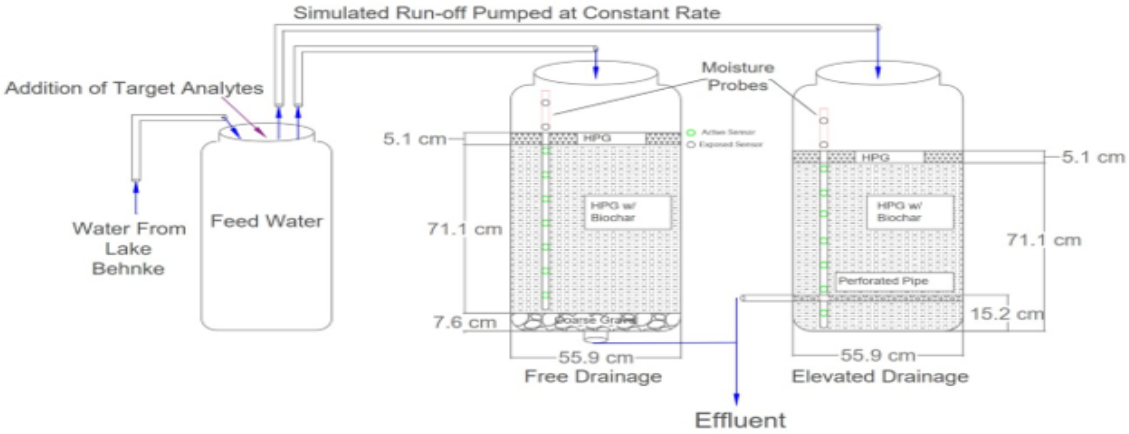


Figure 3. 6 Schematic of pilot scale BRSs.

Then, the two barrels were leveled with a bubble level and ratchet-strapped to the plastic pallet. Urban runoff sourced from Lake Behnke was artificially enriched with ammonium hydroxide (NH4_44OH) and potassium nitrate (KNO3_33) to produce semi-synthetic stormwater.

This resulted in target nitrogen concentrations ranging from approximately 0.8 to 1.0 mg/L as nitrate/nitrite nitrogen (NOx_xx-N), and 0.3 to 0.6 mg/L as ammonium nitrogen (NH4+_4^+4+-N). Prior to formal experimentation, this spiked stormwater solution was applied weekly to both bioretention configurations to promote biofilm development. The simulated storm event schedule closely matched the 10-year design storm intensity-duration-frequency (IDF) curve defined by the Florida Department of Transportation (FDOT, 2022) for Zone 6, where the University of South Florida (USF) is located.

To realistically emulate runoff dynamics from urban catchments, maximum volumetric flow rates were computed using the Rational Method.

A catchment-to-treatment area ratio of 50:1 was assumed, corresponding to a bioretention surface footprint of approximately 2% of the total drainage area (BISBRS footprint).

Additionally, near-total imperviousness typical of small-scale ultra-urban catchments was represented with a runoff coefficient (C-value) of 0.99.



a) Moisture Sensors

Each BIS was equipped with a Bluetooth-enabled Drill & Drop moisture probe (Sentek Technologies, Stepney, SA, Australia), centrally positioned to ensure representative sampling. Each probe incorporated nine individual moisture sensors arranged vertically at 10 cm intervals, providing volumetric soil moisture readings at multiple depths. These detailed measurements allowed for the reconstruction of soil-water profiles, with data acquisition intervals set to a minimum of one minute.

Additionally, these moisture measurements facilitated the estimation of air-filled porosity within the soil media, thereby indirectly indicating the availability of oxygen within the soil column.

For probe management and data handling, the Drill & Drop Connect mobile application was employed to adjust sensor settings and retrieve data wirelessly via Bluetooth. Subsequently, the retrieved data were accessible through the Irrimax Live web-based application for further analysis.

Although the stability of probe connectivity occasionally varied, the acquired data provided consistently high temporal and spatial resolution, ensuring reliable monitoring of moisture dynamics within the systems.

b) Pumps

Water from Mandira Dam, which collects urban runoff from Sundargarh, was pumped into a dedicated mixing tank using a Little Giant 1/6-HP submersible pump. During tank filling, precise volumes of a saturated stock solution containing ammonium chloride and potassium nitrate were introduced to achieve targeted concentrations of approximately 1.0 mg/L nitrate-nitrite nitrogen (NO_x-N) and 0.5 mg/L ammonium nitrogen (NH_4-N).

Thorough mixing of the feed water was ensured through turbulence generated by the inflowing water. Immediately before each experimental run, the homogenized feed water was sampled to confirm consistent nutrient concentrations.

To supply the mixed water to the pilot-scale arrangement, a Pondmaster SP-800 submersible fountain pump was utilized.

The water was delivered via a 1-inch diameter tubing connected to a 360-degree sprinkler head, ensuring uniform distribution over the test system.

Flow rates during individual trials were carefully controlled by selectively opening or sealing perforations in the tubing immediately upstream of the sprinkler head and adjusting the intake area of the pump.

5) Instruments used

a) Sieves and Shaker

Ten standard tests were performed following ASTM specifications to assess media cleanliness and determine particle size distribution.

A set of sieves with mesh openings of 0.250, 0.425, 0.500, 0.600, 1.00, 1.18, 1.14, 2.36, 4.75, and 9.50 mm was used.

These sieves were arranged in order of decreasing size, with a pan at the bottom and a lid on top, then placed in a W.S. Tyler RX-29 shaker (Mentor, OH) to carry out the particle size analysis.

b) Ammonia Analyzer

Effluent water samples collected from the pilot trials were analyzed to determine ammonium (NH_4^+) and nitrate-nitrite (NO_x, defined as the combined concentration of nitrite (NO_2^-) and nitrate (NO_3^-)) concentrations. Analytical measurements were carried out using an ASX-260 autosampler (CETAC Technologies) coupled with a TL-2800 nitrogen analyzer (Timberline Instruments, Boulder, CO).

This instrumentation facilitated precise quantification of nitrogen species, enabling reliable assessment of nutrient removal efficiencies achieved by the pilot-scale treatment systems.

B. Methodology

1) Batch Study

To determine the porosity of the media, a 500 mL sample was placed into a 750 mL beaker, and deionized water was incrementally added using a graduated cylinder until the media appeared fully saturated.

The beaker was then securely sealed with parafilm and allowed to rest undisturbed for 24 hours to ensure complete saturation throughout the sample. Following this equilibration period, additional water was carefully added in small increments until further addition resulted in an increase in the total sample volume, indicating saturation capacity had been reached.

The cumulative volume of water introduced during this process was recorded as the pore volume, representing the effective void space available within the media for water retention. For the particle size distribution analysis, a 200 g sample of the media was placed on a stack of ten sieves arranged in descending mesh sizes. The sieve stack was subjected to mechanical shaking for 10 minutes to facilitate thorough particle separation. After agitation, each sieve was weighed, and the amount of material retained on each was calculated by subtracting the empty sieve weight.

A cumulative mass distribution curve was then created by summing the retained masses sequentially from the finest to the coarsest sieve, and normalizing these values against the total initial mass to obtain the relative distribution.

2) Column Tests

A Constant Head Conductivity test was conducted to measure the unsaturated hydraulic conductivity of both the media mix and the HPG. Water was delivered to each column at a consistent rate using a peristaltic pump.

The flow rate was carefully regulated to maintain a steady inflow, allowing the formation of a stable ponding layer at the top of the column. This ensured a constant hydraulic head, enabling accurate assessment of the column's hydraulic performance. Applying the following equation, saturated hydraulic conductivity was calculated.

$$SaturatedHydraulicConductivity = K_S = \frac{QL}{A\Delta H}$$

where,

Q= Volumetric Flow Rate (cm^3/s)

L= Media Depth (cm)

A= Cross Sectional Area (cm^2)

Δh= Constant Head Difference

After each trial, columns were drained for 48hr to reach field capacity. At each sampling port (and equivalent depth in the HPG-only column), wet samples were collected and weighed, then oven-dried at 104 °C for 24hr and reweighed.

Moisture mass was calculated as the difference between wet and dry weights, converted to volumetric water content by dividing moisture volume by sample volume, and plotted against depth to produce moisture-retention profiles.

3) Pilot Study Methodology

a) Design Storms

The performance of the prototype bioretention system (BRS) was assessed under both typical and extreme precipitation scenarios by selecting two representative design storms: a median-frequency event reflective of local climatological conditions and a storm event with a 10-year recurrence interval. Storm intensities and durations were derived from the Florida Department of Transportation's Zone 6 intensity-duration-frequency (IDF) curves, which are applicable to the University of South Florida (USF) campus, and these parameters were applied using the Rational Method.

The contributing drainage area was assumed to be 50 times the size of the BRS footprint, corresponding to a 2% treatment ratio, and a runoff coefficient (CN) of 0.99 was adopted to simulate highly impervious, ultra-urban conditions.

Owing to limitations in the pumping system's capability to replicate a natural triangular hydrograph, a simplified rectangular hydrograph was employed instead.

This rectangular hydrograph maintained a constant flow rate equivalent to the peak flow predicted by the Rational Method and was applied for half the duration of the corresponding triangular hydrograph, thereby preserving the total runoff volume delivered to the system.

Subsequently, peak flow rates and total runoff volumes were calculated for storm durations of 15, 20, and 30 minutes across return periods of 2, 5, 10, and 25 years (see Table 3.1). The 10-year, 20-minute storm was selected to represent the extreme loading condition, as its hydraulic loading rate aligned with both the experimental design criteria and the operational limitations of the pumping system.

For the typical loading scenario, median storm parameters were derived from four years of rain gauge data collected at the USF campus and analyzed by Hernandez (2001), providing representative values of rainfall intensity and duration.

Table 3. 1 Tabulation of duration, intensity, and peak flows of all considered design storms

Interval	Duration (min)	Intensity (in/hr)	Volume (cuft)	Qpeak (cfs)	Qpeak (gpm)
2 year					
	15	6	14	0.016	6.6
	20	4.5	15.8	0.014	6
	30	3.5	19.8	0.010	4.7
5 year					
	15	5.7	15.7	0.016	7.6
	20	5.1	18.3	0.014	6.6
	30	4.1	23	0.014	5.7
10 year					
	15	6.5	17.4	0.018	8.5
	20	5.5	20.3	0.016	7.4
	30	4.5	25	0.015	6
25 year					
	15	7	18.9	0.022	9.4
	20	6.2	22.9	0.020	7.9
	30	5	28	0.015	6.9
Median Event	30	1.2	5.9	0.004	1.6

©IJRASET: All Rights are Reserved | SJ Impact Factor 7.538 | ISRA Journal Impact Factor 7.894 |

b) Sampling Plan

During each 10-year storm trial, Mandira dam water was collected and pumped into the mixing tank and then delivered to the BRS at 7.4 GPM (0.00046 m^3/s) for 30 minutes. Effluent flow was quantified by timing how long it took to fill a 150 mL bottle with a stopwatch. Samples were collected at the moment effluent first appeared (t = 0) and again at 5, 10, 15, 20, 30, and 40 minutes.

The delay between influent start and initial effluent was recorded, and the antecedent dry period between consecutive events was noted.

To monitor moisture dynamics without excessive power use, probes logged data for one minute during each storm and then once every four hours afterward.

The median-storm protocol followed the same steps, except that the system was fed at 1.5 GPM (9.6×10^{-5} m^3/s) for 30 min, and samples were taken at effluent onset and at 5, 10, 20, 30, and 35 min thereafter.

The NO_x-N and NH_4^+-N concentration analyses was conducted at Environmental lab, Sundargarh. The calibration standards were prepared and detection limits was found to be 0.0567 mg/L for NO_x-N and 0.138 mg/L for NH_4^+-N.

Any measured concentrations falling below these thresholds were substituted with the corresponding detection limit value. A similar study was reported with water-quality parameters by Guimaray 2020 (doctoral dissertation).

3.2.3.3. Data Analysis

For each storm and system combination, hydrographs were developed by calculating the mean flow rate within each sampling interval throughout the event.

The flow rate for each interval was derived by averaging the measured rates at the interval's start and end points, with adjustments made as needed to account for steady-state moisture conditions.

These hydrographs were then utilized to establish mass balances for NH_4^+-N and NO_x-N. Effluent concentrations for each interval were determined by averaging the concentrations measured at the beginning and end of the interval.

Corresponding effluent volumes were calculated by multiplying the interval flow rate by its duration. Subsequently, the percentage mass removal was computed as follows:

$$MassRemoval\ \% = * 100 \frac{V_0C_0 - \sum n1\ CnVn}{V_0C_0}$$

where,

V_0= Influent Volume (Liters)

C_0= Influent Concentration (mg/L)

C_n=Average Concentration of each interval (mg/L) V_n=Effluent Volume of each interval (Liters) n=total number of intervals

To determine the statistical significance of various factors influencing nitrogen mass removal efficiency, a series of single-factor ANOVA tests were performed following the calculation of nitrogen removal values. Specifically,

ANOVA tests were conducted separately using data from the 10-year storm event, the mean storm data, and the combined dataset across all monitored nitrogen species.

These analyses aimed to determine the impact of drainage system design on the removal efficiencies of individual nitrogen species. Additionally,

ANOVA was applied to compare removal efficiencies across different nitrogen species grouped by drainage style, utilizing data from the 10-year storm, median storm data, and the comprehensive dataset. This comprehensive statistical approach allowed clear identification of influential variables and their interactions with system design parameters

IV. RESULTS AND DISCUSSION

A. Media Characterization

1) Bench Scale Results

With a little variance among BCS and BCN, porosity began to rise proportionately as the biochar fraction rose (Table 4.1).

Table 4. 1 Porosity of HPG with varying biochar amendments

Media	Porosity (cm^3/cm^3)
HPG Only	0.44

HPG w/20% BS	0.45
HPG w/30% BS	0.47
HPG w/40% BS	0.49
HPG w/40% Biochar Now	0.5

Because the overall size of biochar was similar to that of HPG media, the amendment produced no apparent influence on the collective behavior of the particle distribution.

Figure 4.1 provides a picture of the largest influences of the amendment below 0.1 inch (0.25 cm) in diameter, and Figure 4.2 is a closer view of the finer range.

Considering that some biochar aggregates fractures into particles, this was to be anticipated. Particle size distribution parameters are shown in Table 4.2.

There was a decrease of 14% in d10 and a decrease of 2% in d6 by the addition of biochar, and uniformity increased by 14%.

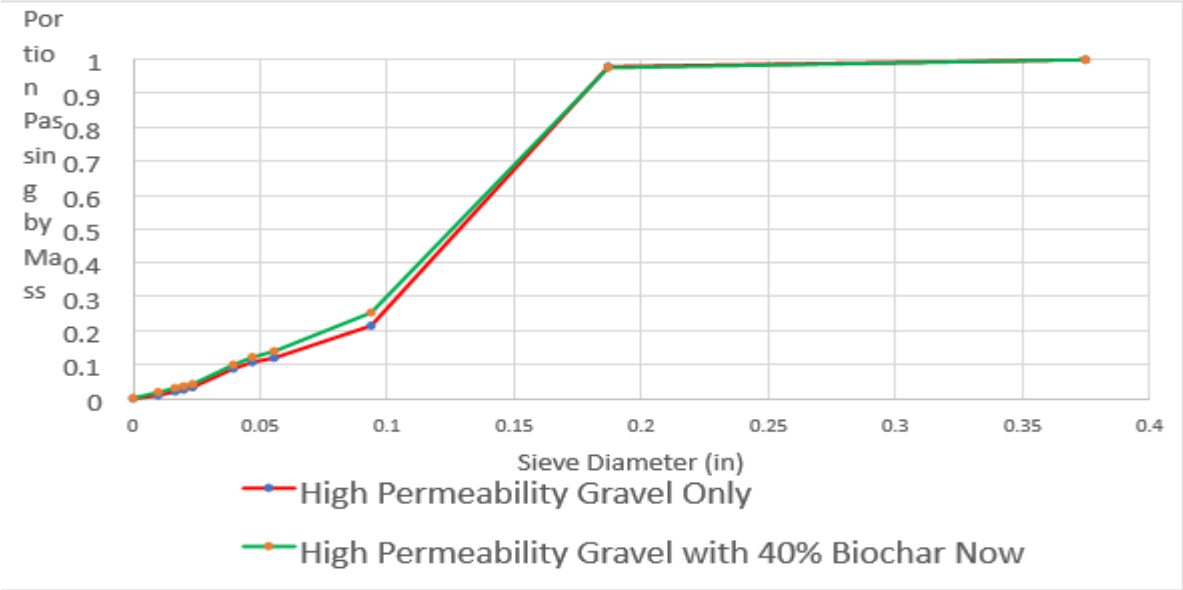


Figure 4. 1 Cumulative particle size distribution of HPG and HPG with 40% volumetric biochar amendment.

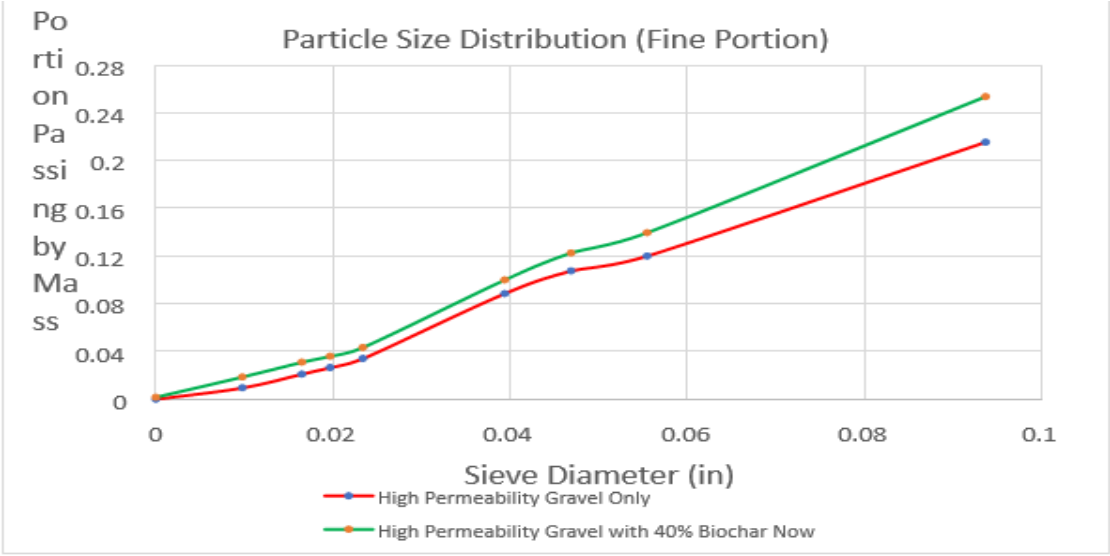


Figure 4.2 Close- up of the particle size distribution highlighting the area of highest difference

Table 4. 2 Particle size distribution parameters

Media	d60	d50	d10	Uniformity
HPG	0.141	0.126	0.0465	3.033
HPG w/ 40% BCN	0.138	0.125	0.0400	3.451

A notable finding was that the addition of biochar disrupted the typical direct correlation between porosity and hydraulic conductivity: despite an increase in porosity, hydraulic conductivity decreased.

This phenomenon is attributed to the nanoporous structure of biochar particles, which enhances total porosity by retaining water within nanopores that do not facilitate flow. Because the water trapped in these nanopores remains essentially immobile—behaving as part of the solid matrixit limits fluid movement through the interconnected pore network, thereby reducing the overall hydraulic conductivity.

B. Column Study

1) Saturated Hydraulic Conductivity

The saturated hydraulic conductivity of the HPG with and without 40% compost by volume was also relatively close; Table 4.3 shows that the amendment lowered the conductivity only slightly, by approximately 5%.

Table 4. 3 Saturated hydraulic conductivities

Media	Ks (cm/s)
High Permeability Gravel	0.78
High Permeability Gravel + 40% Biochar New	0.76

2) Moisture Content

In the free-draining system amended with biochar, field-capacity moisture profiles reveal enhanced water retention, which is further amplified under elevated-drain conditions.

This increase reflects both the development of a perched water tablewith its accompanying capillary fringeand, principally in the raised-drain configuration, sustained saturation within the IWSZ.

Quantitatively, the biochar-amended free-drain column held an additional 3 cm^3 of water per cm of depth compared to the unmodified HPG control. Introducing an elevated drain (but excluding the IWSZ's direct contribution) yielded an extra 2.6 cm^3/cm depth over the amended free-drain column.

These increments were determined by integrating the area under each moisture-content profile (Figure 4.3), then normalizing by column cross-sectional area and depth.

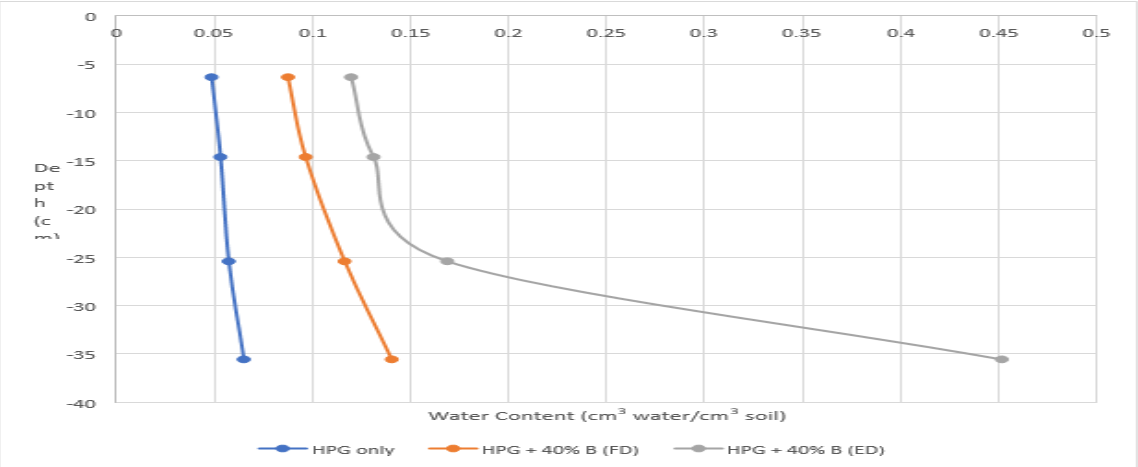


Figure 4.3 Graph of moisture retention vs depth in each column

ISSN: 2321-9653; IC Value: 45.98; SJ Impact Factor: 7.538
Volume 13 Issue VI June 2025- Available at www.ijraset.com

C. Pilot Study Results

1) 10-year Storm N Removal

Figure 4.4 illustrates the average volumetric outflow hydrographs for each system during the 10-year storm simulations, presented alongside the constant influent flow rate of the simulated stormwater.

During the initial phase, both systems quickly reached dynamic equilibrium, with effluent discharge equaling the steady influent rate. Following cessation of the influent flow, effluent rates decreased rapidly over a brief drainage period before gradually declining to zero.

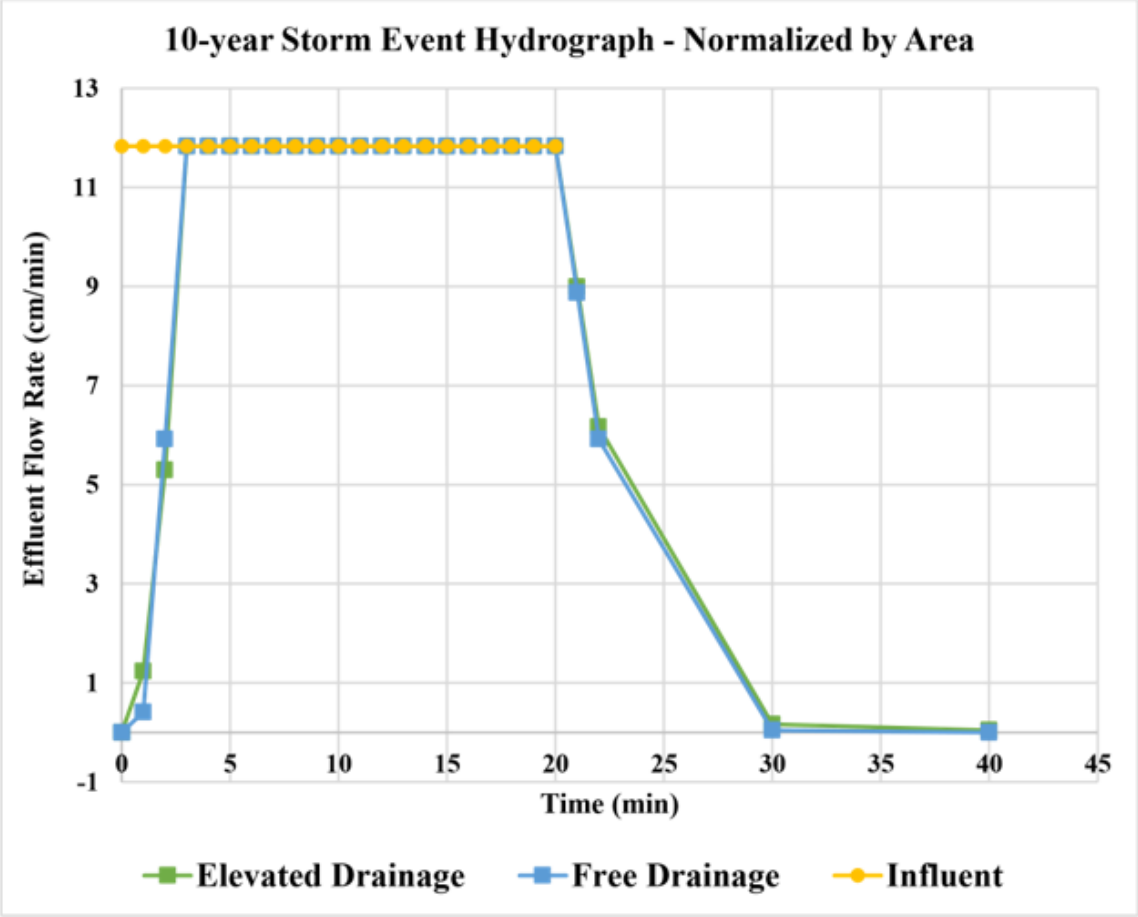


Figure 4. 4 Hydrograph constructed from averaging effluent flowrates across all 10-year event trials

In nearly every 10-year storm trial, both systems hydraulically performed well, smoothly draining runoff with ponding limited to about 5 cm. However, one outlier trial produced roughly 15 cm of ponding.

This anomaly—preventing a definitive conclusion—likely resulted from a shortened antecedent dry period and minor particulate fouling in the feedwater tank. Both the NOx-N and NH4+-N effluent concentration profiles showed similar trends, starting low when flushing out the system's inherent, treated water and peaking when there was steady state infiltration before declining again after infiltration ceased at 20 minutes.

Slower drainage rates allow for extended hydraulic retention time (HRT), which in turn enhances post-infiltration treatment of effluent. Event-based observations, including those from a decade earlier, revealed broadly consistent trends, albeit with some variation in specific parameters.

As expected, the NO_x–N concentration profile in the Raised Drain system generally exhibited lower values compared to the Free Drainage system. This trend aligns with the influence of the internal water storage zone (IWSZ) and the reduced oxygen availability in the soil's air phase under raised drainage conditions, both of which promote denitrification.

Conversely, the NH_4^+–N profile showed higher concentrations in the Raised Drain system and lower values in the Free Drainage system.

©IJRASET: All Rights are Reserved | SJ Impact Factor 7.538 | ISRA Journal Impact Factor 7.894 |

This inverse relationship is consistent with the enhanced oxygen availability in the Free Drainage setup, which supports more efficient nitrification. Representative concentration profiles for both nitrogen species across events are presented in Figures 4.5 and 4.6.

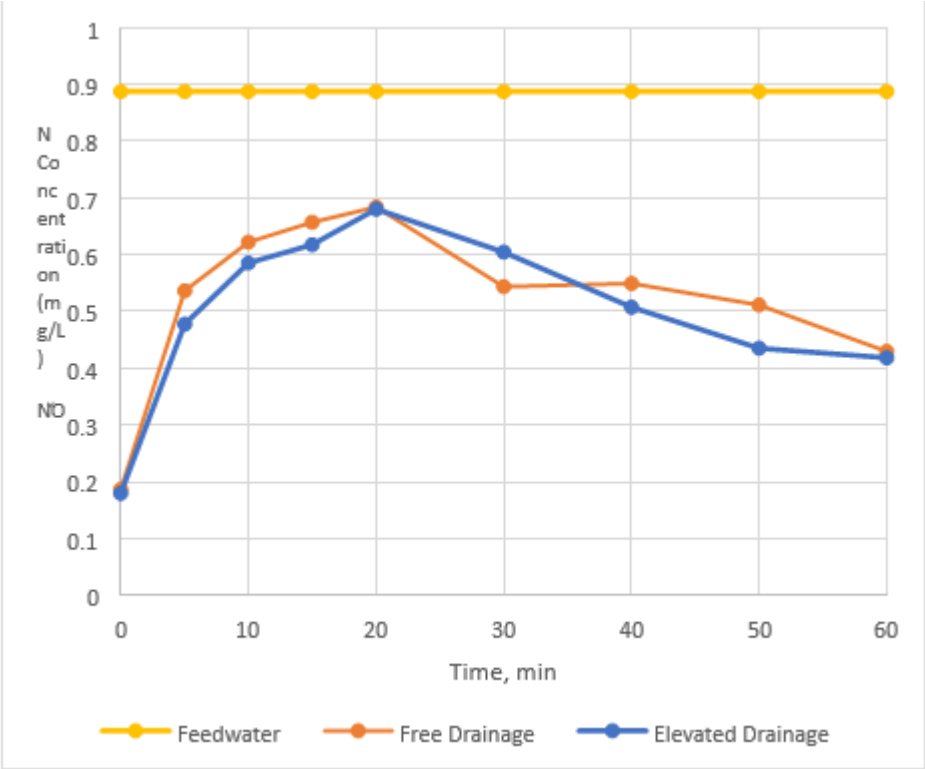


Figure 4. 5 Typical concentration of NO_x-N profile for 10-year infiltration event

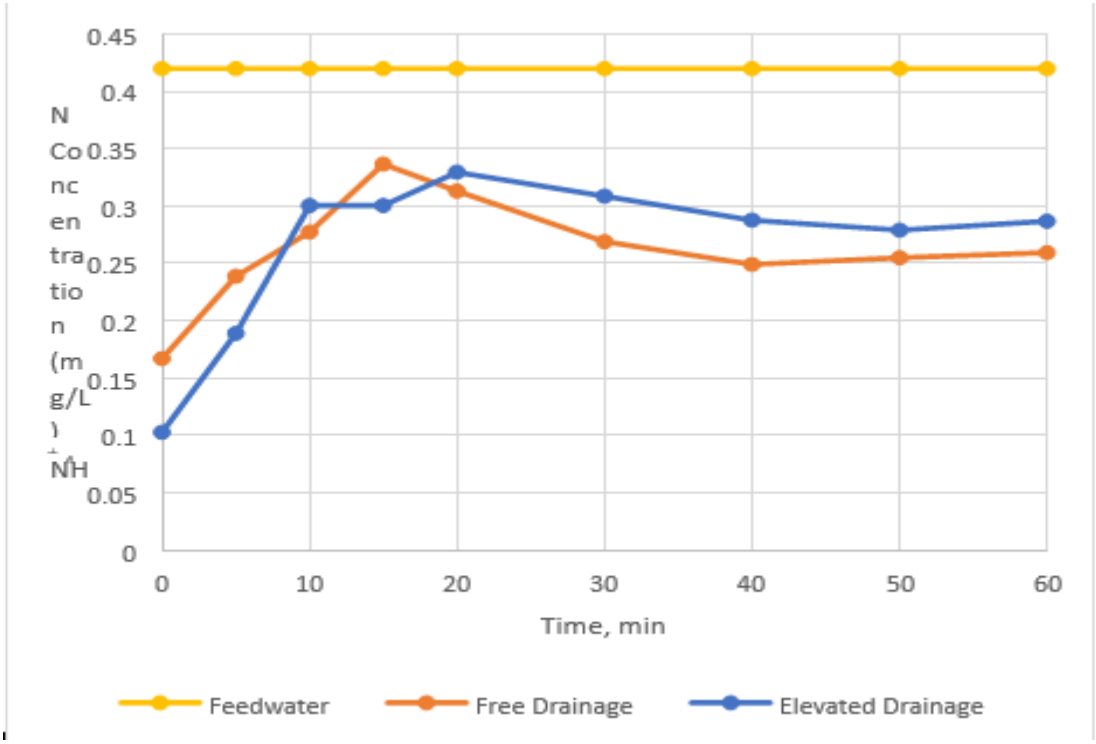


Figure 4. 6 Typical concentration of NH_4^+-N profile during a 10-year infiltration event

ISSN: 2321-9653; IC Value: 45.98; SJ Impact Factor: 7.538
Volume 13 Issue VI June 2025- Available at www.ijraset.com

Total inorganic nitrogen (TIN) removal across both drainage configurations ranged from 15% to 35%. The highest individual removal rate—38%—was recorded for NH_4^+–N in the elevated-drain system, while the lowest was observed for NO_x–N under free-drainage conditions.

With the exception of one outlier trial conducted on February 17, the elevated-drain configuration consistently outperformed the free-drain system in removing NO_x–N, whereas the free-drain setup demonstrated superior removal of NH_4^+–N. Although the elevated-drain system showed a slightly higher overall removal efficiency, the combined removal of TIN (NO_x–N + NH_4^+–N) was nearly identical between the two systems.

This suggests that the rate of denitrification—the only pathway through which nitrogen is permanently removed as dinitrogen gas (N_2)—was comparable in both configurations, despite differences in the removal pathways for individual nitrogen species. Figure 4.7 presents boxplots summarizing the median, range, and interquartile values for nitrogen mass removal efficiency by species and drainage type during the 10-year storm simulations. Table 4.4 presents the corresponding mean values along with their standard deviations, providing a summary of the data variability.

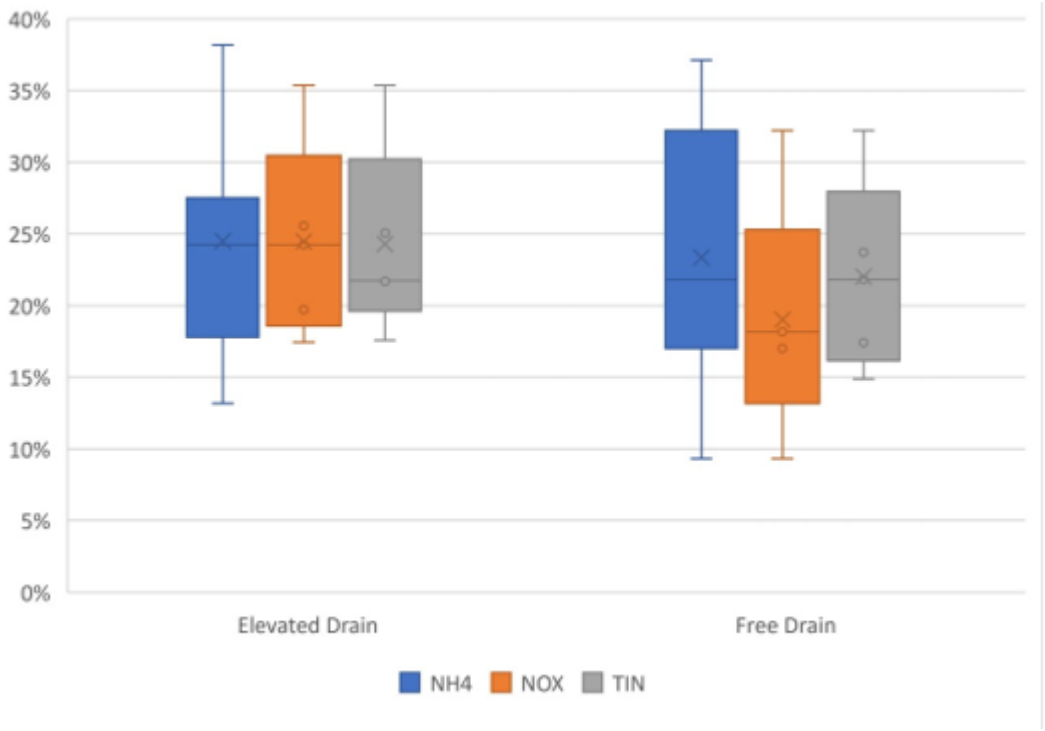


Figure 4. 7 Box plot of mass removal efficiencies for 10-year storm events separated by N species and drain style

Table 4. 4 Tabulation of mass removal efficiency for 10-yr storm event trials

		17-Feb	28-Feb	2-Mar	10-Mar	6-Apr	Avg	Std Dev
NH_4+	Elevated Drain	37%	18%	13%	26%	26%	24%	9.1%
	Free Drain	31%	25%	16%	36%	35%	29%	8.4%
NO_x	Elevated Drain	35%	17%	26%	24%	20%	24%	6.9%
	Free Drain	32%	9.3%	18%	18%	17%	19%	8.2%

©IJRASET: All Rights are Reserved | SJ Impact Factor 7.538 | ISRA Journal Impact Factor 7.894 |

TIN	Elevated Drain	37%	17%	21%	26%	22%	23%	7.1%
	Free Drain	31%	16%	18%	23%	22%	21%	6.7%

2) 10-year Storm Moisture Content Profile

Figure 4.8 presents a comparison of soil moisture profiles measured by the probes under field-capacity and steady-state infiltration conditions.

During steady-state flow, the raised-drain system demonstrated nearly uniform saturation throughout the media profile, fostering optimal conditions for denitrification by sustaining anoxic zones favorable to microbial processes.

In contrast, the free-drainage system stabilized at roughly 40 % volumetric water content, maintaining substantial air-filled porosity that favors nitrification.

Throughout the infiltration trials, the free-drain column never became fully saturated and, during post-storm drainage, retained less moisture overall, facilitating rapid oxygen replenishment in its pore network and further promoting aerobic nitrogen transformation.

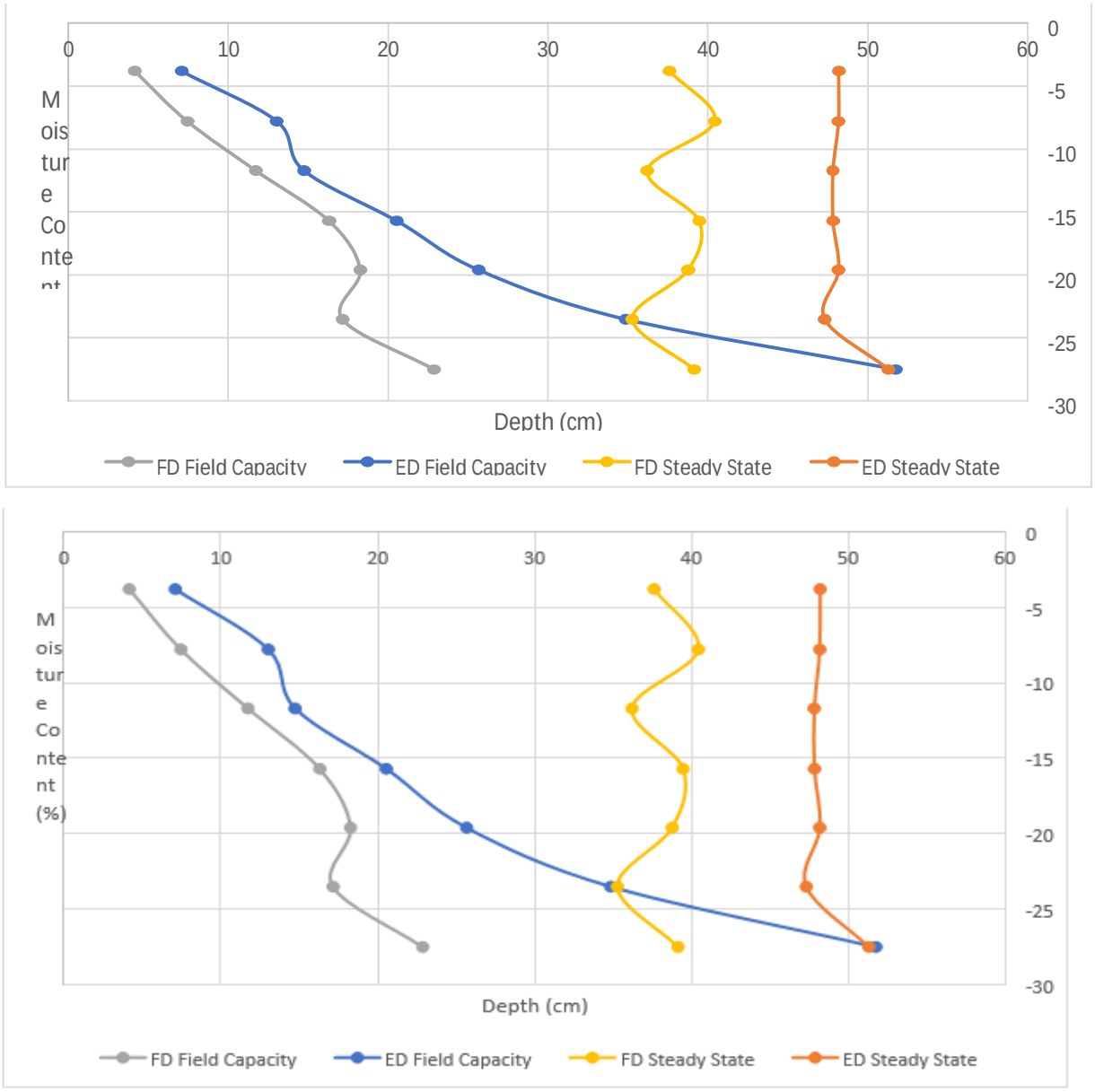


Figure 4. 8BRS moisture content profiles at field capacity and under steady state infiltration

To estimate the nitrogenous oxygen demand (NOD) during the 10-year storm event, a stoichiometric factor of 3.55 was applied to the mean ammonium-nitrogen (NH_4^+–N) load of 228 mg N, yielding an NOD of approximately 810 mg O_2.

The total gas-phase oxygen content in each column was estimated by calculating the air-filled pore volume (i.e., total porosity minus moisture at field capacity), then multiplying by the volumetric fraction of oxygen in air (0.21) and the standard density of oxygen at STP (1,427 g/m³).

This calculation yielded total oxygen volumes of approximately 8,750 mg O_2 in the free-drain column and 5,490 mg O_2 in the raised-drain column, both substantially exceeding the estimated nitrogenous oxygen demand (NOD) under field-capacity conditions. However, under steady-state infiltration, the gas-phase oxygen content decreased significantly due to increased saturation. In this case, the raised-drain column retained only around 480 mg O_2—approximately 60% of the NOD—whereas the free-drain system maintained approximately 2,600 mg O_2. This disparity explains the more anaerobic environment within the internal water storage zone (IWSZ) of the raised-drain system, in contrast to the relatively oxygen-rich conditions of the free-drain configuration. Notably, during drainage following storm events, as the media returns to field capacity, the IWSZ allows for the passive reintroduction of atmospheric oxygen—estimated at roughly 5,000 mg—helping sustain nitrification between storms by preventing prolonged oxygen limitation.

The incorporation of biochar significantly enhanced the soil moisture retention profile, and this effect was further amplified by the presence of an IWSZ. These conditions supported the development of microbial biofilms in both systems, facilitating nitrogen transformation processes.

While further exploration of this effect is anticipated in Joshelyn Guimaray's forthcoming doctoral dissertation, preliminary observations—such as the frequent need for surface weeding between storm events—suggest that elevated moisture levels may also promote plant growth. Importantly, while the surface IWSZ helped maintain higher moisture levels that could theoretically support increased denitrification, the observed improvement in denitrification was modest, indicating that other factors may be limiting.

4.3.3. Median Storm Nitrogen Removal

Figure 4.9 illustrates the average effluent flow patterns for the two drainage setups during the median-storm tests, shown alongside the steady influent flow rate. At the lower hydraulic loading rate (2.4 cm/s), both systems showed a slower response, taking more time to saturate and reach a stable outflow. This contrasts with their quicker stabilization observed at the higher loading rate of 11.8 cm/s during the simulated 10-year storm event.

This extended time to steady-state reflects the slower infiltration dynamics and increased storage potential associated with lower-intensity rainfall events. Moreover, the performance gap between the free-drain and raised-drain systems becomes more pronounced under these gentler loading conditions. Because the free drainage system contains less moisture in its profile, it requires more water to reach saturation and takes on average 4 minutes longer to achieve steady state due to this. Both systems' flow rates decreased quickly after the influent ceased flowing, with the free drainage system having a slightly more rapid decrease before flowrates approached nearly zero. Surface ponding was not present in all trials of a median storm event.

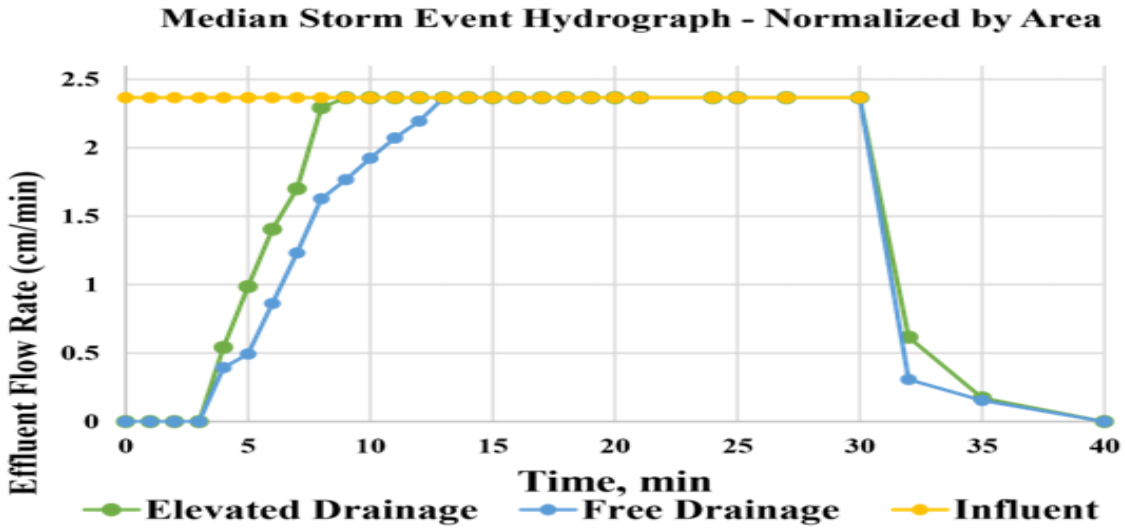


Figure 4. 9 Hydrograph from averaging effluent flow rates across all median event *trials*

Compared Relative to the 10-year storm, effluent NO_x-N and NH_4^+-N concentrations during the median event were more variable and lacked the uniform plateau seen under extreme loading.

Both systems exhibited an initial dilution spike—albeit less pronounced—followed by a relatively flat concentration trend, reflecting constant HRT since saturation was never achieved.

As before, the raised-drain configuration produced lower NO_x-N levels than the free-drain system at most sampling points, and the same pattern held for NH_4^+-N. Figures 4.10 and 4.11 show representative effluent concentration profiles for both nitrogen species.

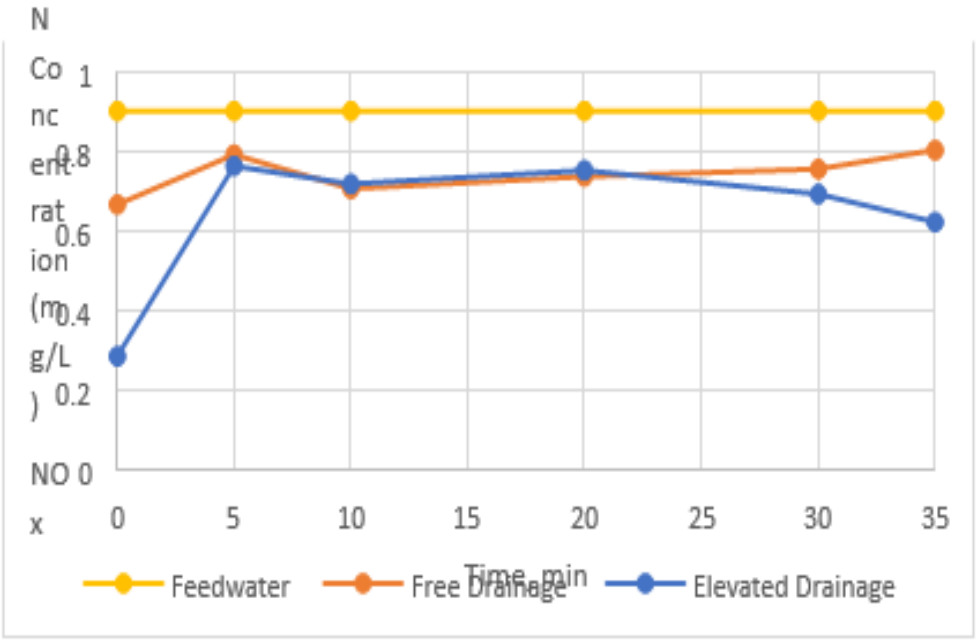


Figure 4. 10 Typical concentration of NOx-N profile during a median infiltration event

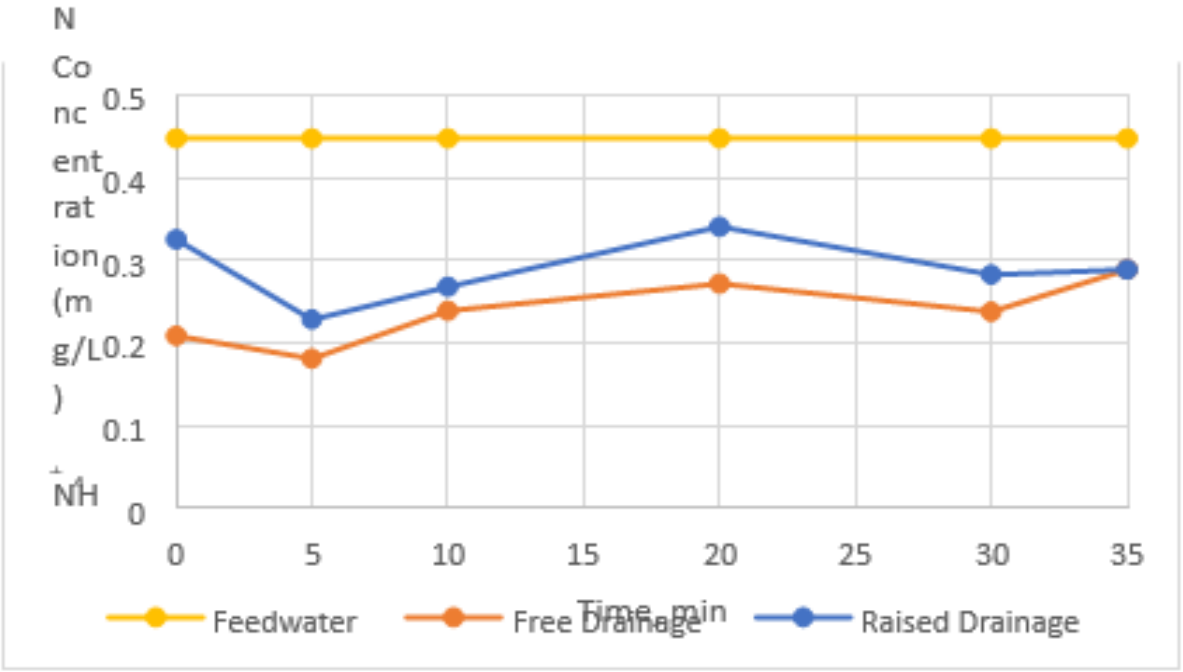


Figure 4. 11 Typical concentration of NH_4^+-N profile during a median infiltration event

Figure 4.12 presents boxplots depicting the range, standard deviation, and mass removal efficiencies for each nitrogen species across both drainage configurations during the median-storm trials.

These visual summaries highlight the variability and central tendencies in treatment performance for NH_4^+–N and NO_x–N under moderate loading conditions.

The corresponding numerical values, including means and standard deviations, are provided in Table 4.5 for reference and comparison.

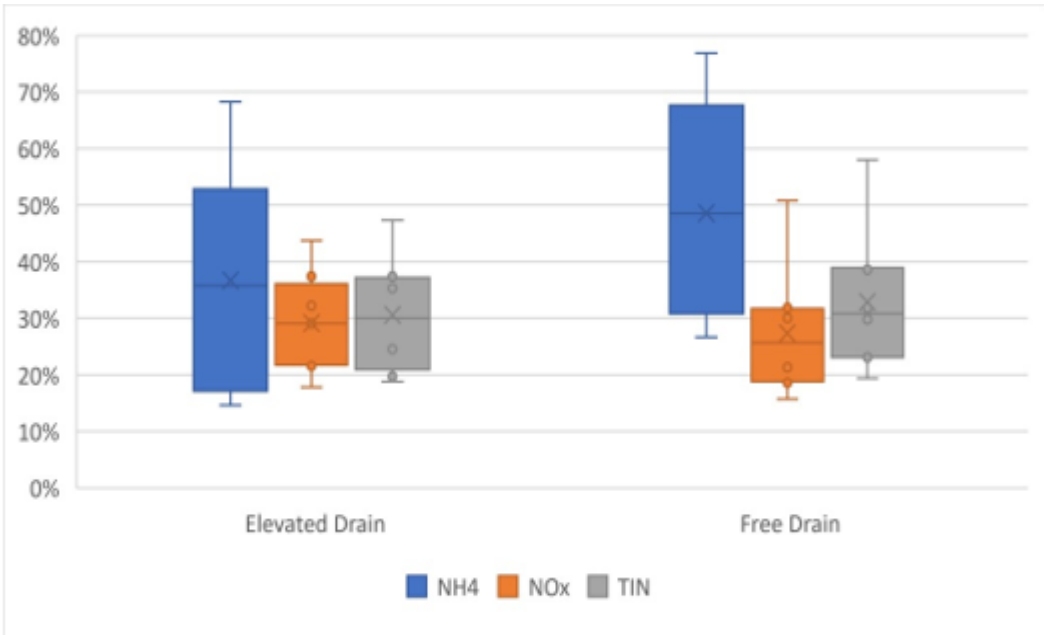


Figure 4. 12 Box plot of mass removal efficiencies for median storm events separated by nitrogen species and drain style

Table 4. 5 Tabulation of mass removal efficiency for median storm event trials

		16-May	18-May	23-May	25-May	30-May	6-June	13-June	20-June	Average	Std Dev
NH_4+	Elevated Drain	54%	41%	30%	15%	21%	48%	16%	61%	36%	20%
	Free Drain	72%	53%	46%	27%	31%	52%	31%	74%	48%	17%
NOX	Elevated Drain	45%	33%	21%	21%	19%	28%	28%	38%	28%	10%
TIN	Free Drain	51%	31%	21%	16%	19%	30%	19%	32%	27%	6.8%
	Elevated Drain	47%	35%	25%	20%	19%	37%	25%	45%	32%	14%
	Free Drain	58%	39%	30%	19%	23%	39%	23%	45%	35%	10%

3) Mass Removal Discussion

The study's findings are encouraging. Betz et al. (2023) achieved average removals of 79 % NH_4^+-N and 9 % NO_3^--N in a small-scale system—and 45 % NH_4^+-N and 28 % NO_3^--N in a larger one—operating at highly variable HLRs on the order of 0.01–1 cm/min. Despite our systems running at substantially higher HLRs (11.8 and 2.4 cm/min), we observed comparable nitrogen removal. Kong et al. (2024), using mixed pyrite, woodchip, and charcoal media at 0.0145 cm/min, reported 96 % NH_4^+-N, 79 % NO_3^--N, and 86 % TIN removal (minimum TIN removal = 64 %).

all exceeding our 72 %, 51 %, 58 %, and 15 % figures. Similarly, Tian et al. (2019) observed nitrate removal efficiencies between 30.6% and 95.7% at a hydraulic loading rate of 0.091 cm/min in media systems amended with both iron and biochar, highlighting the effectiveness of these amendments in enhancing denitrification performance.

The broad spectrum of HLRs—and especially the scarcity of high-rate data in previous work—makes direct comparison difficult. Subjecting systems like ours to a wider HLR range would clarify their loading-rate sensitivity and better contextualize performance against existing studies.

Figure 4.13 offers a comprehensive visual summary of mass removal efficiencies across all trials, broken down by nitrogen species (NO_x^-, NH_4^+, TIN), storm intensity (10-year vs. median), and drain configuration (elevated vs. free). Because TIN removal quantifies the permanent conversion of nitrogen to N_2, it remains the most relevant indicator of system efficacy.

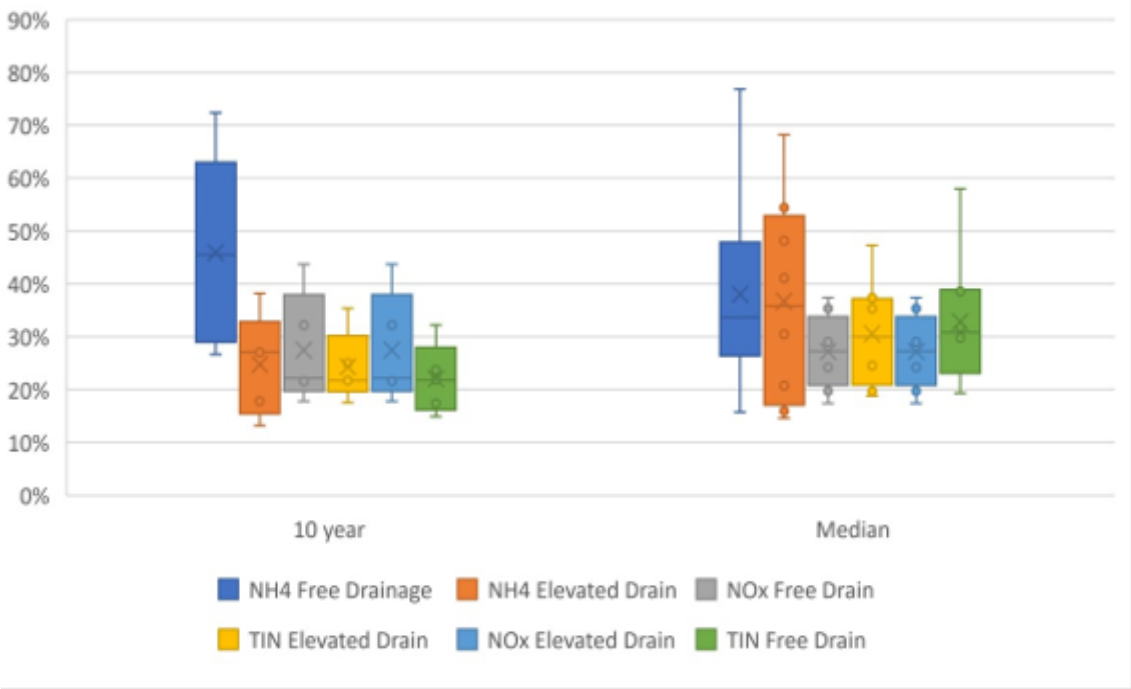


Figure 4. 13 Box plot of mass removal efficiencies from all trials, separated by all relevant parameters

ANOVA results (Table 4.6) revealed four p-values below the 0.05 threshold, each comparing NH_4^+ removal to NO_x removal.

During the median storm, the free-drain configuration yielded p = 0.0167, and when both systems were pooled, p = 0.0134. Across both storm events, the free-drain system produced p = 0.0083,

while combining both systems gave p = 0.0087—an order of magnitude more significant. In every scenario, NH_4^+ removal was favored over NO_x, with the free-drain setup showing the strongest preference.

This preference for ammonium removal, especially in the free-drain system, represents the study's most statistically robust finding.

Table 4. 6 Tabulation of P values for single variable ANOVA tests comparing mass removal efficiencies by N-species and drain style

Drain Style: Free vs Elevated			
	10 year storm	Median storm	All storms
NH_4^+	0.433	0.197	0.173
NOx	0.290	0.728	0.402
TIN	0.585	0.625	0.834
N-Species Removal: NH_4^+ vs NOx			
	10 year storm	Median storm	All storms

Elevated	0.931	0.358	0.434
Free	0.108	0.017	0.008
Both	0.230	0.015	0.010

V. CONCLUSION AND RECOMMENDATIONS

The selection of drainage type should be based on site-specific conditions such as peak flow rates and influent concentration ratios of ammonia to nitrate, but more research is needed to completely comprehend which to implement by monitoring the specific impacts of IWSZ depth and size. These systems can be the first step in a treatment train for water quality treatment and ought to be an effective passive storm water quantity treatment in urban catchments.

The study's primary hypothesis is confirmed: both systems effectively processed high-rate HLR runoff, but achieved even greater dissolved-nitrogen removal—approximately 30%—under the lower, more typical HLR representative of real storm events, rather than the <20% removal seen at extreme loading.

These mass-removal results indicate that biochar amendments to high-permeability media offer a promising urban storm water treatment strategy.

Moreover, the free-draining configuration consistently removed more NH_4^+—indicative of enhanced nitrification—while the elevated-drain system preferentially removed NO_x—reflecting denitrification—thereby supporting our secondary hypothesis that free-drain BRSs favour nitrification and elevated-drain BRSs favour denitrification.

Total inorganic nitrogen (TIN) removal did not differ significantly between free- and elevated-drain configurations for either design storm, indicating that denitrification—the sole permanent nitrogen-removal pathway—occurred at similar rates in both systems. Drain style thus had negligible influence on overall dissolved-N removal and no statistically significant effect on species-specific targeting.

In contrast, storm intensity exerted a clear influence: average TIN reduction was 34 % under the median-event HLR versus 23 % under the 10-year storm HLR (11.8 cm/min).

VI. ACKNOWLEDGEMENT

It is with immense pleasure that I express my sincere sense of gratitude andhumble appreciation to Prof. Sanam Sarita Tripathy for his invaluable guidance, whole-heartedco-operation,constructivecriticismandcontinuousencouragementinthepreparation of this thesis. Without his support and guidance, the present work wouldhaveremained adream.

I would also like to thank Prof. Surajit Pattnaik, HOD Civil, GIFT Autonomous forprovidingnecessaryfacilities.

I take this opportunity to thank all my scholar friends & family for theirvaluable support and encouragement throughout the preparation of this work. I alsothankall those who havedirectlyor indirectlyhelped in completion of this work.

REFERENCES

[1] Ahlfeld, D. P., & Minihane, M. (2004). Storm Flow from First-Flush Precipitation in Stormwater Design. *Journal of Irrigation and Drainage Engineering*, *130*(4), 269-276. https://doi.org/doi:10.1061/(ASCE)0733-9437(2004)130:4(269)

[2] Ali, W., Takaijudin, H., & Yusof, K. W. (2021). The Role of Bioretention Plant on Nutrient Removal of Stormwater Runoff. IOP Conference Series: Earth and Environmental Science,

[3] Betz, C., Ament, M. R., Hurley, S. E., & Roy, E. D. (2023). Nitrogen removal performance in roadside stormwater bioretention cells amended with drinking water treatment residuals. Journal of Environmental Quality, 52(6), 1115-1126. https://doi.org/https://doi.org/10.1002/jeq2.20506

[4] Biswal, B. K., Vijayaraghavan, K., Adam, M. G., Lee Tsen-Tieng, D., Davis, A. P., & Balasubramanian, R. (2022). Biological nitrogen removal from stormwater in bioretention cells: a critical review [Review]. *Critical Reviews in Biotechnology*, *42*(5), 713-735. https://doi.org/10.1080/07388551.2021.1969888

[5] Brown, R. A., & Hunt, W. F. (2009). Effects of media depth on bioretention performance in the upper coastal plain of North Carolina and bioretention construction impacts study. Proceedings of World Environmental and Water Resources Congress 2009 - World Environmental and Water Resources Congress 2009: Great Rivers,

[6] Brown, R. A., & Hunt, W. F. (2011). Evaluating media depth, surface storage volume, and presence of an internal water storage zone on four sets of bioretention cells in North Carolina. World Environmental and Water Resources Congress 2011: Bearing Knowledge for Sustainability - Proceedings of the 2011 World Environmental and Water Resources Congress,

[7] Brown, R. A., & Hunt, W. F. (2011). Impacts of Media Depth on Effluent Water Quality and Hydrologic Performance of Undersized Bioretention Cells [Article]. *Journal of Irrigation and Drainage Engineering*, *137*(3), 132-143. https://doi.org/10.1061/(ASCE)IR.19434774.0000167

©IJRASET: All Rights are Reserved

[8] Brown, R. A., & Hunt, W. F. (2011). Underdrain Configuration to Enhance Bioretention Exfiltration to Reduce Pollutant Loads. *Journal of Environmental Engineering*, *137*(11), 1082-1091. https://doi.org/doi:10.1061/(ASCE)EE.1943-7870.0000437

[9] Burns, M., Fletcher, T., Walsh, C., Ladson, A., & Hatt, B. (2012). Hydrologic shortcomings of conventional urban stormwater management and opportunities for reform. *Landsc Urban Plan*, *105*. https://doi.org/10.1016/j.landurbplan.2011.12.012

[10] Davis, A. P., Shokouhian, M., Sharma, H., & Minami, C. (2006). Water quality improvement through bioretention media: Nitrogen and phosphorus removal [Article]. *Water Environment Research*, *78*(3), 284-293. https://doi.org/10.2175/106143005X94376

[11] Ding, S. M., Chen, M. S., Gong, M. D., Fan, X. F., Qin, B. Q., Xu, H., Gao, S. S., Jin, Z. F., Tsang, D. C. W., & Zhang, C. S. (2018). Internal phosphorus loading from sediments causes seasonal nitrogen limitation for harmful algal blooms [Article]. *Science of the Total Environment*, *625*, 872-884. https://doi.org/10.1016/j.scitotenv.2017.12.348

[12] Donaghue, A. G., Beganskas, S., & McKenzie, E. R. (2022). Inverted versus Raised: The Impact of Bioretention Underdrain Height on Internal Water-Storage Hydraulics [Article]. *Journal of Sustainable Water in the Built Environment*, *8*(1), Article 04021024. https://doi.org/10.1061/JSWBAY.0000974

[13] Donaghue, A. G., Beganskas, S., & McKenzie, E. R. (2022). Inverted versus Raised: The Impact of Bioretention Underdrain Height on Internal Water-Storage Hydraulics [Article]. *Journal of Sustainable Water in the Built Environment*, *8*(1), Article 04021024. https://doi.org/10.1061/JSWBAY.0000974

[14] Donaghue, A. G., Morgan, N., Toran, L., & McKenzie, E. R. (2022). The impact of bioretention column internal water storage underdrain height on denitrification under continuous and transient flow [Article]. *Water Research*, *214*, Article 118205. https://doi.org/10.1016/j.watres.2022.118205

[15] Douglas, I. (2020). URBAN HYDROLOGY. In *The Routledge Handbook of Urban Ecology: Second Edition* (pp. 164-185). Taylor and Francis. https://doi.org/10.4324/9780429506758-16

[16] Du, S., Shi, P., Van Rompaey, A., & Wen, J. (2015). Quantifying the impact of impervious surface location on flood peak discharge in urban areas. *Natural Hazards*, *76*(3), 14571471. https://doi.org/https://doi.org/10.1007/s11069-014-1463-2

[17] Egodawatta, P., & Goonetilleke, A. (2008). Modelling pollutant build-up and wash-off in urban road and roof surfaces. In M. Lambert, T. Daniell, & M. Leonard (Eds.), *Water Down Under 2008: Proceedings of the 31st Hydrology and Water Resources Symposium and the 4th International Conference on Water Resources and Environment Research* (pp. 418-427). Engineers Australia. https://eprints.qut.edu.au/13708/

[18] Guan, M. F., Sillanpaa, N., &Koivusalo, H. (2016). Storm runoff response to rainfall pattern, magnitude and urbanization in a developing urban catchment. *Hydrol Process*, *30*.

[19] Hathaway, J. M., Tucker, R. S., Spooner, J. M., & Hunt, W. F. (2012). A traditional analysis of the first flush effect for nutrients in stormwater runoff from two small urban catchments [Article]. *Water, Air, and Soil Pollution*, *223*(9), 5903-5915. https://doi.org/10.1007/s11270-012-1327-x

[20] Hsieh, C. H., & Davis, A. P. (2005). Evaluation and optimization of bioretention media for treatment of urban storm water runoff [Article]. *Journal of Environmental Engineering*, *131*(11), 1521-1531. https://doi.org/10.1061/(ASCE)0733-9372(2005)131:11(1521)

[21] Huang, L., Luo, J., Li, L., Jiang, H., Sun, X., Yang, J., She, W., Liu, W., Li, L., & Davis, A. P. (2022). Unconventional microbial mechanisms for the key factors influencing inorganic nitrogen removal in stormwater bioretention columns. *Water Research*, *209*, 117895. https://doi.org/https://doi.org/10.1016/j.watres.2021.117895

[22] Kong, Z., Song, Y., Xu, M., Yang, Y., Wang, X., Ma, H., Zhi, Y., Shao, Z., Chen, L., Yuan, Y., Liu, F., Xu, Y., Ni, Q., Hu, S., & Chai, H. (2024). Multi-media interaction improves the efficiency and stability of the bioretention system for stormwater runoff treatment. Water Research, 250, 121017. https://doi.org/https://doi.org/10.1016/j.watres.2023.121017

[23] Kinney, T. J., Masiello, C. A., Dugan, B., Hockaday, W. C., Dean, M. R., Zygourakis, K., & Barnes, R. T. (2012). Hydrologic properties of biochars produced at different temperatures. *Biomass and Bioenergy*, *41*, 34-43. https://doi.org/https://doi.org/10.1016/j.biombioe.2012.01.033

[24] Laurenson, G., Laurenson, S., Bolan, N., Beecham, S., & Clark, I. (2013). The Role of Bioretention Systems in the Treatment of Stormwater. In *Advances in Agronomy* (Vol. 120, pp. 223-274). Academic Press Inc. https://doi.org/10.1016/B978-0-12-407686-0.00004-X

[25] Lehmann, J. (2007). Bio-energy in the black. *Frontiers in Ecology and the Environment*, *5*(7), 381-387. https://doi.org/https://doi.org/10.1890/1540-9295(2007)5[381:BITB]2.0.CO;2

[26] Liu, J., Sample, D., Bell, C., & Guan, Y. (2014). Review and research needs of bioretention used for the treatment of urban stormwater. *Water*, *6*. https://doi.org/10.3390/w6041069

[27] Luo, H., Guan, L., Jing, Z., He, B., Cao, X., Zhang, Z., & Tao, M. (2020). Performance evaluation of enhanced bioretention systems in removing dissolved nutrients in stormwater runoff [Article]. *Applied Sciences (Switzerland)*, *10*(9), Article 3148. https://doi.org/10.3390/app10093148

[28] Luo, Y., Yue, X., Duan, Y., Zhou, A., Gao, Y., & Zhang, X. (2020). A bilayer media bioretention system for enhanced nitrogen removal from road runoff [Article]. *Science of the Total Environment*, *705*, Article 135893. https://doi.org/10.1016/j.scitotenv.2019.135893

[29] McGrane, S. J. (2016). Impacts of urbanisation on hydrological and water quality dynamics, and urban water management: a review. *Hydrol Sci J-J Sci Hydrol*, *61*. https://doi.org/10.1080/02626667.2015.1128084

[30] Miguntanna, N. P., Liu, A., Egodawatta, P., & Goonetilleke, A. (2013). Characterising nutrients wash-off for effective urban stormwater treatment design [Article]. *Journal of Environmental Management*, *120*, 61-67. https://doi.org/10.1016/j.jenvman.2013.02.027

[31] Nair, P. K. R. (2002). The Nature and Properties of Soils, 13th Edition.By N. C. Brady and R. R. Weil. *Agroforestry Systems*, *54*(3), 249-249. https://doi.org/10.1023/A:1016012810895

[32] Nazarpour, S., Gnecco, I., & Palla, A. (2023). Evaluating the Effectiveness of Bioretention Cells for Urban Stormwater Management: A Systematic Review [Review]. *Water (Switzerland)*, *15*(5), Article 913. https://doi.org/10.3390/w15050913

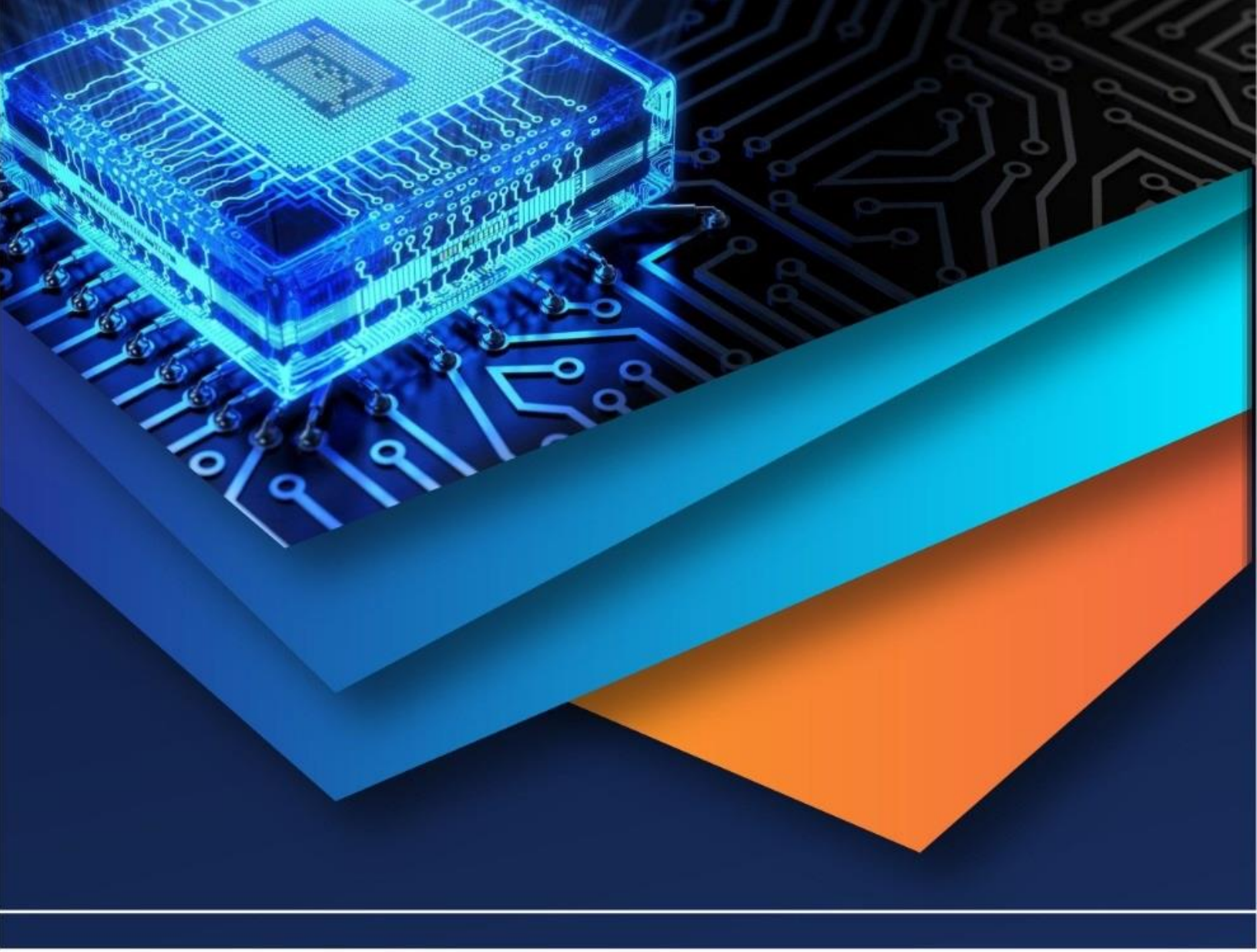
[33] Phlips, E. J., Badylak, S., Mathews, A. L., Milbrandt, E. C., Montefiore, L. R., Morrison, E. S., Nelson, N., & Stelling, B. (2023). Algal blooms in a river-dominated estuary and nearshore region of Florida, USA: the influence of regulated discharges from water control structures on hydrologic and nutrient conditions [Article]. Hydrobiologia, 850(20), 4385-4411. https://doi.org/10.1007/s10750-022-05135-w

[34] Ray, C., Bezak, B., Petrey, K., & Shea, E. (2015). Measurement and optimization of permeability in bioretention soil media. International Low Impact Development Conference 2015 - LID: It Works in All Climates and Soils - Proceedings of the 2015 International Low Impact Development Conference,

[35] Reddy, K. R., Dastgheibi, S., &Cameselle, C. (2021). Mixed versus layered multi-media filter for simultaneous removal of nutrients and heavy metals from urban stormwater runoff [Article]. *Environmental Science and Pollution Research*, *28*(6), 7574-7585. https://doi.org/10.1007/s11356-020-11120-4

[36] Roodsari, B. K., & Chandler, D. G. (2017). Distribution of surface imperviousness in small urban catchments predicts runoff peak flows and stream flashiness [Article]. *Hydrological Processes*, *31*(17), 2990-3002. https://doi.org/10.1002/hyp.11230
[37] Skaugen, T., Lawrence, D., & Ortega, R. Z. (2020). A parameter parsimonious approach for catchment scale urban hydrology – Which processes are important? [Article]. *Journal of Hydrology X*, *8*, Article 100060. https://doi.org/10.1016/j.hydroa.2020.100060
[38] Tian, J., Jin, J., Chiu, P. C., Cha, D. K., Guo, M., & Imhoff, P. T. (2019). A pilot-scale, bi-layer bioretention system with biochar and zero-valent iron for enhanced nitrate removal from stormwater. Water Research, 148, 378-387. https://doi.org/https://doi.org/10.1016/j.watres.2018.10.030
[39] Timberline Instruments. (2010). <Microsoft Word - TL-2800 Instruction Manual 121310.doc - TL2800InstructionManual-1.pdf>.
[40] Trowsdale, S. A., & Simcock, R. (2011). Urban stormwater treatment using bioretention [Article]. *Journal of Hydrology*, *397*(3-4), 167-174. https://doi.org/10.1016/j.jhydrol.2010.11.023
[41] Vaze, J., & Chiew, F. H. S. (2004). Nutrient Loads Associated with Different Sediment Sizes in Urban Stormwater and Surface Pollutants. *Journal of Environmental Engineering*, *130*(4), 391-396. https://doi.org/doi:10.1061/(ASCE)0733-9372(2004)130:4(391)
[42] Wang, Z., Sedighi, M., R. Lea-Langton, A., & Babaei, M. (2022). Hydraulic behaviour of sandbiochar mixtures in water and wastewater treatment applications. *Journal of Hydrology*, *612*, 128220. https://doi.org/https://doi.org/10.1016/j.jhydrol.2022.128220
[43] Wright, O. M., Istanbulluoglu, E., Horner, R. R., DeGasperi, C. L., & Simmonds, J. (2018). Is there a limit to bioretention effectiveness? Evaluation of stormwater bioretention treatment using a lumped urban ecohydrologic model and ecologically based design criteria [Article]. *Hydrological Processes*, *32*(15), 2318-2334. https://doi.org/10.1002/hyp.13142
[44] Wurtsbaugh, W. A., Paerl, H. W., & Dodds, W. K. (2019). Nutrients, eutrophication and harmful algal blooms along the freshwater to marine continuum [Article]. *Wiley Interdisciplinary Reviews-Water*, *6*(5), 27, Article e1373. https://doi.org/10.1002/wat2.1373
[45] Yang, H., McCoy, E. L., Grewal, P. S., & Dick, W. A. (2010). Dissolved nutrients and atrazine removal by column-scale monophasic and biphasic rain garden model systems [Article]. *Chemosphere*, *80*(8), 929-934. https://doi.org/10.1016/j.chemosphere.2010.05.021
[46] Zart, D., Stüven, R., & Bock, E. (2008). Nitrification and Denitrification-Microbial Fundamentals and Consequences for Application. In *Biotechnology: Second, Completely Revised Edition* (Vol. 11-12, pp. 55-64). Wiley-VCH Verlag GmbH. https://doi.org/10.1002/9783527620999.ch3l
[47] Zhang, H., Ahmad, Z., Shao, Y., Yang, Z., Jia, Y., & Zhong, H. (2021). Bioretention for removal of nitrogen: processes, operational conditions, and strategies for improvement [Review]. *Environmental Science and Pollution Research*, *28*(9), 10519-10535. https://doi.org/10.1007/s11356-020-12319-1

©IJRASET: All Rights are Reserved | SJ Impact Factor 7.538 | ISRA Journal Impact Factor 7.894 |



10.22214/IJRASET

45.98

IMPACT FACTOR: 7.129

IMPACT FACTOR: 7.429

INTERNATIONAL JOURNAL FOR RESEARCH

IN APPLIED SCIENCE & ENGINEERING TECHNOLOGY

Call : 08813907089 (24*7 Support on Whatsapp)